

Pre- and post-inspiratory neurons change their firing properties in female rats exposed to chronic intermittent hypoxia

George M.P.R. Souza,^{a,*} William H. Barnett,^b Mateus R. Amorim,^a Ludmila Lima-Silveira,^a Davi J.A. Moraes,^a Yaroslav I. Molkov^b and Benedito H. Machado^a

^aDepartment of Physiology, School of Medicine of Ribeirão Preto, University of São Paulo, Ribeirão Preto, SP, Brazil

^bDepartment of Mathematics and Statistics & Neuroscience Institute, Georgia State University, Atlanta, GA, United States of America

Abstract—Obstructive sleep apnea patients face episodes of chronic intermittent hypoxia (CIH), which has been suggested as a causative factor for increased sympathetic activity (SNA) and hypertension. Female rats exposed to CIH develop hypertension and exhibit changes in respiratory–sympathetic coupling, marked by an increase in the inspiratory modulation of SNA. We tested the hypothesis that enhanced inspiratory-modulation of SNA is dependent on carotid bodies (CBs) and are associated with changes in respiratory network activity. For this, in CIH-female rats we evaluated the effect of CBs ablation on respiratory–sympathetic coupling, recorded from respiratory neurons in the working heart–brainstem preparation and from NTS neurons in brainstem slices. CIH-female rats had an increase in peripheral chemoreflex response and in spontaneous excitatory neurotransmission in NTS. CBs ablation prevents the increase in inspiratory modulation of SNA in CIH-female rats. Pre-inspiratory/inspiratory (Pre-I/I) neurons of CIH-female rats have a reduced firing frequency. Post-inspiratory neurons are active for a longer period during expiration in CIH-female rats. Further, using the computational model of a brainstem respiratory–sympathetic network, we demonstrate that a reduction in Pre-I/I neuron firing frequency simulates the enhanced inspiratory SNA modulation in CIH-female rats. We conclude that changes in respiratory–sympathetic coupling in CIH-female rats is dependent on CBs and it is associated with changes in firing properties of specific respiratory neurons types. © 2019 IBRO. Published by Elsevier Ltd. All rights reserved.

Key words: respiratory neurons, carotid bodies, chronic intermittent hypoxia, sympathetic activity.

INTRODUCTION

Intermittent episodes of hypoxia are a hallmark of obstructive sleep apnea (OSA) and are considered one of the causative factors of autonomic disorders associated with this disease such as sympathetic overactivity and hypertension (Somers et al., 1995; Narkiewicz et al., 1998a; Caples et al., 2005). There is evidence suggesting that carotid bodies (CBs) tonicity in OSA patients contributes to the increased muscle peroneal sympathetic nerve activity (MSNA) and hypertension (Narkiewicz et al., 1998b). These conclusions were based on the findings that acutely silencing CBs with hyperoxia (100% of O₂ inhaled) leads to a reduction in MSNA and blood pressure (BP) in OSA patients but not in control subjects (Narkiewicz et al., 1998b).

In rats, the acute activation of CBs promotes a significant increase in sympathetic nerve activity (SNA) and BP (Franchini

and Krieger, 1993; Braga et al., 2006; Tubek et al., 2016). Chronic intermittent activation of CBs by chronic intermittent hypoxia (CIH) contributes to the development of neurogenic hypertension in male rats (Fletcher et al., 1992; Prabhakar et al., 2005; Del Rio et al., 2016; Nanduri et al., 2018). In fact, CIH-male rats present an enhancement of SNA response to acute CBs activation, indicating changes in the neural circuitry involved in processing this reflex (Braga et al., 2006; Costa-Silva et al., 2012). These evidences indicate that CIH induces an enhancement of peripheral chemoreflex sensitivity in male rats, which is likely to contribute to the increased SNA and development of hypertension in this experimental model (Del Rio et al., 2016; Nanduri et al., 2018).

Hypertension induced by CIH is associated with an enhancement of the respiratory modulation of SNA in male and female rats, which is marked by an increase in inspiratory modulation of SNA in CIH-female rats and in expiratory modulation of SNA in CIH-male rats (Zoccal et al., 2008; Souza et al., 2015, 2016, 2017). Changes in the respiratory and sympathetic coupling in CIH-male rats are dependent on CBs integrity during the onset of CIH (Moraes and Machado, 2015) but acute ablation of CBs after the CIH

*Corresponding author at: Department of Pharmacology, University of Virginia, PO Box 800735, 1300 Jefferson Park Avenue, Charlottesville, VA 22908-0735, USA.
E-mail address: gs4bd@virginia.edu (George M.P.R. Souza).

protocol does not attenuate the increased sympathetic activity (Zoccal et al., 2008). In this context, we investigated whether physiological responses to CIH conditioning in female rats were dependent on CBs integrity; we evaluated the SNA response to acute peripheral chemoreflex activation and the inspiratory modulation of SNA after CBs ablation using the working heart brainstem preparation of rats (WHBP). Information arising from CBs is first processed by the nucleus of solitary tract (NTS) neurons at the brainstem, an important synaptic station of the peripheral chemoreflex neural pathway (Finley and Katz, 1992; Machado, 2001). To test if CIH enhances the excitatory neurotransmission at the level of NTS in female rats, we additionally recorded spontaneous excitatory post-synaptic currents (sEPSC) from NTS neurons.

Experimental evidences indicate that the respiratory–sympathetic coupling occurs due to the modulation of pre-sympathetic neurons by the respiratory network at the medulla (Haselton and Guyenet, 1989; Moraes et al., 2013). CIH induces changes at the level of respiratory and sympathetic brainstem network activities, which could explain an increase of the respiratory modulation of SNA (Moraes et al., 2013; Moraes and Machado, 2015; Machado et al., 2017). CIH-male rats exhibit a significant increase in the activity of specific subsets of expiratory neurons at the ventral medulla, which may contribute to modulate the firing frequency of pre-sympathetic neurons at the late-expiration (Machado et al., 2017).

Taking into consideration that changes in respiratory pattern and in respiratory–sympathetic coupling in CIH-female rats are phase-locked to inspiration, we aimed to evaluate whether these animals present changes in the firing properties of inspiratory neurons. We hypothesized that inspiratory neurons in the brainstem respiratory circuitry have changed their firing pattern to support this phenomenon. To test this hypothesis, we systematically evaluated the firing properties of inspiratory and expiratory neurons at the ventral medulla using the extracellular single unit recordings in the WHBP of CIH-female rats, which constitute an intact brainstem network free of the effect of anesthesia.

Additionally, we performed simulations of brainstem neural circuitry including the respiratory central pattern generator of Böttinger and pre-Böttinger complexes and pre-sympathetic circuitry of the ventrolateral medulla. Using the refined computational model based on our previous publications (Baekey et al., 2010; Molkov et al., 2010, 2011; Rybak et al., 2012; Molkov et al., 2017; Barnett et al., 2017, 2018), we show how inspiratory neurons of the pre-Böttinger complex may shape respiratory modulation in the sympathetic output and also how CIH-induced plasticity in neurons of the pre-Böttinger complex may alter respiratory modulation in the sympathetic output of female rats. Taken together, the present study demonstrates the effects of CBs stimulation in producing changes in the respiratory and sympathetic network activity and identifies changes in the firing properties of specific respiratory neuron subtypes that are likely to be associated with the changes of respiratory–sympathetic network after CIH in female rats.

EXPERIMENTAL PROCEDURES

Ethical approval

All the experimental protocols were approved by the institutional ethical committee of the School of Medicine of Ribeirão Preto, USP (Protocol # 091/2013) and are in accordance with the principle that this Journal operates. Juvenile female Wistar rats (P20–P21) were provided by the animal care facility of University of São Paulo, Ribeirão Preto, Brazil. We used 44 animals for the carotid body ablation protocol, 40 for the extracellular single unit recordings protocols and 12 for the NTS whole-cell patch clamp recordings. Juvenile female rats used in this study are sexually immature and does not present estral cycle. During the protocol, rats were kept in Plexiglas chambers with food and water provided *ad libitum* and light–dark cycle of 12 h. The decerebrated preparations from rats were killed by turning off the perfusion pump after the experiments.

Chronic intermittent hypoxia (CIH)

Rats were kept inside Plexiglas chambers and were exposed to intermittent hypoxia ($F_{I}O_2 = 6\%$) or normoxia ($F_{I}O_2 = 20.8\%$) for 10 days as previously described by Souza et al. (2016). Intermittent hypoxia protocol consisted of lowering the $F_{I}O_2$ inside the chamber from 20.8% to 6% by N_2 injection. Hypoxia episodes lasted about 30 s and after this period, O_2 was injected into the chamber to bring the $F_{I}O_2$ back to 20.8%. The coordination of gases injection into the chamber was automatically controlled by a solenoid valves system (Oxycycler, Biospherix, USA). Episodes of hypoxia occurred every 9 min for 8 h per day (8:00 a.m.–4:00 p.m.). All the electrophysiological recordings were conducted on the day after the last day of CIH protocol similarly as in previous studies using *in vivo* and *in situ* approaches (Souza et al., 2015, 2016).

The level of hypoxia used in this CIH model ($F_{I}O_2 = 6\%$) produces a reduction in oxygen saturation (SaO_2) to the approximate level of 80%, according to Shortt et al. (2014) and Lee et al. (2009). This magnitude of reduction in SaO_2 is comparable to those observed in OSA patients (Sasaki et al., 2018). However, one important aspect of the CIH model used in these experiments is that it does not mimic all features observed in OSA patients, such as hypercapnia during the obstructive event. In the CIH model instead, rats present hypocapnia during the hypoxia episode due to the increase in pulmonary ventilation, once there is no obstruction in the upper airways.

Ventral approach of the working heart–brainstem preparation for extracellular single unit recordings

For the extracellular single unit recordings of respiratory neurons the working heart–brainstem preparation (WHBP) was performed with a ventral medullary surface approach as previously described (Moraes et al., 2014). Rats were deeply anesthetized with halothane (5%, AstraZeneca) and decerebrated at mid-collicular level. The level of anesthesia before decerebration was monitored by the absence of any withdrawal reflex in response to a firm tail pinching. Afterwards, rats were hemi-sectioned, skinned and had the lungs removed. For medullary ventral surface

exposure, trachea, muscles below, the occipital bone were removed using tweezers and then the meninges were carefully removed. After the surgery, rats were taken for the perfusion chamber where they were arterially perfused with a modified aCSF (containing, mM: 10 glucose, 125 NaCl, 1.25 KH₂PO₄, 3 KCl, 24 NaHCO₃, 1.25 MgSO₄, 2.5 CaCl₂ and 1.25 MgSO₄), pH = 7.4 and an oncotic agent (1.25% polyethylene glycol, molecular weight 20.000 g mol⁻¹; Sigma, St Louis, MO, USA). The perfusion pressure (PP) was measured with a double-lumen catheter connected to a pressure transducer and an amplifier (AVS, São Carlos, Brazil). PP was kept constant (50–80 mmHg) by adjusting the flow on tip of catheter (23–25 ml min⁻¹) using a peristaltic pump (Watson-Marlow 502 s, Falmouth, UK) and as soon as the perfusion started, Vasopressin (600–1200 pM) was added to the perfusate. A neuromuscular blocker (Vecuronium bromide, 3–4 µg ml⁻¹; Cristália Produtos Químicos Farmacêuticos Ltda, São Paulo, Brazil) was added to the perfusate to stop the respiratory muscle-related movements and allow optimal electrophysiological recordings. The aCSF was continuously heated (30–31 °C) and gassed with a carbogenic mixture (95% O₂ and 5% CO₂, White-Martins, Sertãozinho, Brazil) as described previously (Souza et al., 2016).

Carotid body ablation before and after CIH

To address the role of carotid bodies (CBs) in the increase of the inspiratory modulation of sympathetic activity in female rats exposed to CIH, we performed the surgical removal of CBs. CBs were surgically removed in two different times: in one group CBs were removed before the onset of CIH (CBx) and in a distinct group CBs were removed after the CIH protocol (Ac-CBx). To remove CBs before the onset of CIH, juvenile female rats were anesthetized with ketamine (40 mg kg⁻¹) and xylazine (5 mg kg⁻¹, Aldrich, Milwaukee, WI, USA). The lack of withdrawal reflex in response to a firm tail pinching was used to evaluate the level of anesthesia during the surgical procedure. A supplementary dose of anesthetic (half of the initial dose) was injected when the rats presented any signal of recovery of withdrawal reflex. When the rats were anesthetized properly, we performed a midline incision in the anterior part of the neck and the carotid bifurcation was visualized. The CB artery was ligated and cut and the CBs were removed bilaterally (Amorim et al., 2016). After the surgery, an analgesic (1 mg kg⁻¹; Banamine; Schering-Plough, Rio de Janeiro, Brazil) and 0.1 ml of antibiotic (1.2 million i.u., Pentabiotic Veterinarian; Fort Dodge, Campinas, Brazil) were given i.m. (Amorim et al., 2016, 2017). The efficacy of CBs removal was confirmed in all rats by the lack of respiratory and sympathetic responses after the injection of potassium cyanide (KCN, 40 µg per rat) as previously described (Amorim et al., 2017). The rats included in this protocol did not present increase in F_R or tSNA in response to KCN injection.

Respiratory and sympathetic nerve recordings in the WHBP

Left phrenic (PN), abdominal (Abd) and thoracic sympathetic nerves (tSNA) were isolated, cut distally and recorded

using a suction glass microelectrode (Souza et al., 2016; Amorim et al., 2017). Ramping pattern and regular frequency of PN bursts were an index of eupneic-like breathing pattern and only preparations that present these characteristics were used in these experiments. Signals were band-pass filtered (0.01–5 kHz), amplified (A-M system), acquired in an A/D converter (CED 1401; Cambridge Electronic Design) and digitized using Spike2 software (Cambridge Electronic Design). The burst of PN was considered as inspiration and the silent part as expiration. Respiratory and sympathetic responses to peripheral chemoreflex were evaluated using the intra-arterial injection of KCN (40 µg per rat).

Extracellular single unit recordings in the working heart–brainstem preparation

Extracellular single unit recordings of respiratory neurons were performed using a glass microelectrode filled with 3 M of NaCl (3–12 MΩ). The electrode was mounted in a pipette holder which was positioned above the ventral surface coupled to a manual 3-D micromanipulator. The electrode was connected to an amplifier and then to A/D converter (Axopatch 200B, Molecular Devices). The signals recorded were low-pass filtered (2 kHz) and digitalized (10 kHz) (CED 1401, CED) to a computer using Spike 2 software (CED). The tip of electrode was introduced into the ventral surface in steps of ~2 µm manually until the extracellular activity was identified. Respiratory neuronal recordings were performed exclusively within ventral surface of medulla in a region comprising the Böttinger (BötC) and pre-Böttinger (Pre-BötC) complexes or in the case of late-expiratory neurons (Late-E) in the region of RTN/pFRG. For anatomical orientation we used the hypoglossal roots, the basilar artery and the trapezoid body which are visually identified in the ventral approach of WHBP (Moraes et al., 2012b, 2014). The stereotaxic parameters of the recording site were 1500–1700 µm lateral from the basilar artery, 500–1000 µm caudal from the caudal pole of trapezoid body and 500 µm ventral–dorsal of maximum depth similar to described previously (Moraes et al., 2012b).

We recorded from Late-E neurons to test the hypothesis that this subpopulation of neurons is silent during resting conditions (normocapnia) in CIH-female rats because this gender does not develop active expiration after CIH, as described by Souza et al. (2016). For the Late-E neurons recordings at the RTN/pFRG we used 1500–1700 µm lateral from the basilar artery, 0–500 µm caudal from the caudal pole of trapezoid body and 100 µm of maximum ventral–dorsal depth (Moraes et al., 2012a,b).

Medullary slices and whole-cell patch clamp recordings from NTS neurons

Considering that NTS is the first synaptic station that receives inputs from CBs and have neurons that project to the ventral respiratory column, we evaluate the synaptic transmission within NTS neurons. These experiments were conducted in medullary slices of CIH and control female

rats. The aim of this experimental protocol was to evaluate the sEPSCs in NTS neurons. The brainstem slices from female rats were obtained after 10 days of CIH or control protocols. For this purpose, rats were decapitated, and the brainstem was exposed and rapidly removed and submerged in ice-cold (~ 0 °C) aCSF solution containing (in mM): 125 NaCl, 2.5 KCl, 1 MgCl₂, 1.25 NaH₂PO₄, 25 NaHCO₃, 25 glucose and 2 CaCl₂, constantly bubbled with 95% O₂ and 5% CO₂ for oxygenation and maintenance of pH at 7.4. Brainstem transversal slices (250 μ m thick) were cut using an oscillating slicer (Vibratome VT1200S plus, Leica Biosystems) and kept in aCSF at 31 °C for 30 min. Thereafter the slices were kept in a solution at room temperature (23–25 °C) in aCSF. For patch-clamp experiments a single slice was submerged into the recording chamber equipped with a temperature controller (TC-324B/344B, Warner Instruments, USA) and it was perfused with aCSF bubbled with carbogenic mixture (flow rate of 2–3 ml min) at 31 °C. A Fixed-Stage Upright Microscope (model BX51WI, Olympus, Japan) was used to visualize the NTS neurons in brainstem slices.

Whole-cell recordings were made using patch pipettes pulled from thick-walled borosilicate glass capillaries (Sutter Instruments, Novato, USA), using a horizontal puller (P-97, Sutter Instruments) and were filled with solution containing (in mM): 130 K-gluconate, 20 KCl, 2 Mg-ATP, 0.3 Na-ATP, 10 Na₂phosphocreatin, 5 EGTA, 10 HEPES. The osmolality of solution was ~ 310 mOsm/Kg-H₂O and pH 7.4 adjusted with KOH. The sEPSCs were recorded under voltage-clamp (-56 mV holding potential) after 5 min of obtaining whole-cell recording configuration. The signals were acquired using an amplifier Multiclamp 700B (Molecular Devices, Sunnyvale, EUA) connected to a data acquisition system (DIGIDATA 1440, Molecular Devices, Sunnyvale, EUA). The software pClamp 10 (Molecular Devices, EUA) was used for signal acquisition and data analysis. Series resistance was checked regularly during the experiments, and cells presenting large variations (20%) or series resistance greater than 30M Ω were discarded.

We selected for records those neurons with healthy appearance located in the commissural aspect of the NTS. This region was chosen based on several neuroanatomical and functional studies showing that the processing of the peripheral chemoreflex occurs mainly at this aspect of the NTS (Finley and Katz, 1992; Chitravanshi et al., 1994; Colombari et al., 1996; Machado, 2001; Accorsi-Mendonca et al., 2011; Accorsi-Mendonca and Machado, 2013). To investigate the sEPSCs all the experiments were performed in presence of Picrotoxin (100 μ M), an antagonist of the GABA receptors, which was added to the bath in order to isolate excitatory currents (Accorsi-Mendonca et al., 2015).

Data analysis

Respiratory–sympathetic coupling

For the respiratory–sympathetic coupling analysis we performed the waveform averages of 10 consecutive respiratory cycles. Considering that these recordings are

multifiber, tSNA activity was quantified as the average between two time points and expressed as relative percentage to the tSNA peak during a respiratory cycle and to the electrical noise (Zoccal et al., 2008; Costa et al., 2013; Souza et al., 2016; Amorim et al., 2017). We considered the maximum tSNA activity (*i.e.* peak of tSNA integrated activity) during a respiratory cycle as 100% and the noise, recorded after the death of preparation, as zero. Additionally, we analyzed the average tSNA activity during each phase of respiratory cycle, during INSP (coincident with PN burst), during E-1 (first half of expiration) and E-2 (second half of expiration) as previously described by Souza et al. (2016).

Spontaneous excitatory post-synaptic currents (sEPSC) in NTS neurons

The sEPSCs were recorded for 1 min in the voltage clamp configuration (-56 holding potential). The currents features were analyzed using the MiniAnalysis program (Synaptosoft Inc., Decatur, USA). To assure an accurate evaluation of the synaptic events, all the currents were selected manually. The MiniAnalysis generated a summary table, where we obtained the frequency, amplitude and half-width of the sEPSCs from each cell. The experimenter was blinded in relation to group treatment.

Characterization of VLM respiratory neuron types

Respiratory neurons were identified and classified according to their firing properties and their time relationship with PN discharge. All neurons considered for the analysis presented phasic activity (*i.e.* they fired in a period of respiratory cycle and complete silenced in another). Seven distinct types of respiratory neurons, four inspiratory and three expiratory related neurons were identified in juvenile female rats according to their firing properties. The inspiratory neurons were characterized by their activity in phase with the PN discharge. Additionally, inspiratory neurons were divided in ramping-inspiratory (Ramp-I), late-inspiratory (Late-I), early-inspiratory (Early-I) and pre-inspiratory/inspiratory (Pre-I/I) neurons according to their firing pattern (Richter and Smith, 2014). We considered Ramp-I as those neurons presenting an augmenting firing frequency and that fired during the whole inspiratory phase. Early-I neurons presented a decrementing firing frequency starting from the beginning to the end of inspiration. Late-I neurons were characterized by their discharge exclusively at the end of inspiration (last half of inspiration). Pre-I/I neurons were characterized by their low frequency activity before the PN discharge, an increase in the firing frequency during inspiration and a complete silencing in the post-inspiratory period.

Expiratory neurons were characterized by their activity exclusively during expiratory period, being completely silenced during PN discharge. Post-inspiratory (Post-I) neurons start to fire immediately after the cessation of PN activity in a decrementing fashion during the expiratory period. Augmenting-expiratory (Aug-E) neurons fired immediately before the onset of PN activity in an augmenting fashion during late-expiration. Late-E neurons were found in the

RTN/pFRG region and their discharge pattern was in phase with active expiration (increase in abdominal nerve activity) in the late-expiratory phase of the respiratory cycle. These latter neuron subtypes were active during hypercapnia ($\text{CO}_2 = 10\%$) and silent in normocapnia ($\text{CO}_2 = 5\%$).

Statistical analysis

Statistical analysis was performed using the software GraphPad Prism 7.01. Data are presented as mean \pm SD and all the variables were tested for normality using Kolmogorov–Smirnov test. The results presenting normal distribution were tested using Student's *t* test and those data that did not present a normal distribution were tested using Mann–Whitney non-parametric test. Two-way ANOVA was used to analyze the effect of CBx and CIH on the respiratory and sympathetic activities. Differences were considered significant when $p < 0.05$.

Computational model

The respiratory circuitry in our computational model was adapted from Barnett et al. (2018) which was in turn derived from Molkov et al. (2011). The pre-sympathetic circuitry and its interconnection with the brainstem respiratory network in the model presented here were adapted from Baekey et al. (2010). In our simulations of the respiratory central pattern generator (CPG), neuronal populations are identified by their phase of activity in the respiratory pattern: inspiration (Early-inspiratory (Early-I) and Pre-inspiratory/inspiratory (Pre-I/I)), post inspiration (Post-inspiratory (Post-I)), and late expiration (Augmenting expiratory (Aug-E)). The spatial and functional organization of the CPG is based on pontine and medullary transection experiments presented in Smith et al. (2007) and modeled in Smith et al. (2007) and Abdala et al. (2007). As such, the three-phase respiratory rhythm is organized by mutual inhibition among the Early-I, Post-I, and Aug-E populations (Fig. 12; Table 1). The inhibitory Post-I population here represents a functional aggregation of heterogeneous expiratory neurons (both inhibitory) being: 1) Post-I neurons that fire in the post-inspiratory phase but not in the late expiration phase and 2) Post-I neurons that fire more strongly during the post inspiration phase but persist for the duration of expiration. This population is modeled as a functionally homogeneous inhibitory population that

fires strongly during the post inspiration phase and then reduces during the late expiration phase. Separately, we consider an excitatory post inspiratory population [Post-I (e)] which participates in pattern formation in the pre-sympathetic circuitry but does not participate in rhythm generation.

Each simulated neuron was described as a single compartment Hodgkin–Huxley type neuron, and each population contained either 20 or 50 neurons. Select biophysical parameters were drawn from a gaussian distribution in order to promote heterogeneity. In all neuron populations, the standard deviation of the distribution of the leak reversal potential was 0.01 mV with the exception of the Pre-I/I population which was 0.02 mV. In the Pre-I/I population the standard deviation of the distribution for the maximal conductance of the persistent sodium current was 0.1 nS. Synaptic projections between populations were all-to-all, and projections from drive elements encompassed all neurons in the target populations. Neuron population output was represented as a spike time histogram with a time bin size of 30 ms. PN and sympathetic (SN) motoneuron outputs were computed by integrating their excitatory neuronal input.

Numerical simulations were performed using NSM 3.0 developed by S. Markin, I. Rybak, and N. Shevtsova (Rybak et al., 2004; Abdala et al., 2007) and then adapted for use in high-performance computing clusters by Y. Molkov (Molkov et al., 2010, 2011, 2013). Solutions to ordinary differential equations were computed using the exponential Euler method with an integration time step of 0.1 ms.

Model adjustments

The principal advancement to our computational model is in the organization of the pre-sympathetic circuitry. This circuitry including the rostral ventrolateral medullary (RVLM) population and a phase-spanning pontine population (IE) was adapted from Baekey et al. (2010). In this model, the excitatory inputs to the RVLM are the IE and pattern forming post-I (e) populations respectively of the pons and Bötzing complex. The inhibitory inputs to the RVLM are from the post-I population that is the integral part of the respiratory CPG, and from the caudal VLM (CVLM) population. Neurons in the CVLM display a diverse repertoire of firing

Table 1. Connectivity of computational model.

Target Population	Excitatory Drive [weight of synaptic input] or Presynaptic Source Population [weight of synaptic input from single neuron]
Aug-E (BötC) ^a	Drive (Pons) [1.2]*; Drive (RTN) [1.5]*; Early-I (1) (Pre-BötC) [−0.135]; Post-I (BötC) [−0.3]
Early-I (1) (pre-BötC) ^a	Drive (Pons) [0.6]; Drive (RTN) [2]; Aug-E (BötC) [−0.265]; Post-I (BötC) [−0.45]; Pre-I/I (pre-BötC) [0.05]
Early-I (2) (rVRG) ^a	Drive (Pons) [2.5]; Aug-E (BötC) [−0.25]; Post-I (BötC) [−0.75]*
Post-I (BötC) ^a	Drive (Pons) [1.45]*; Early-I (1) (Pre-BötC) [−0.025]
Post-I (e) (BötC) ^a	Early-I (2) (pre-BötC) [−0.5]*
Pre-I/I (pre-BötC) ^a	Drive (Pons) [0.45]*; Drive (RTN) [0.22]*; Drive (Raphe) [0.15]; Aug-E (BötC) [−0.01]; Post-I (BötC) [−0.19]; Pre-I/I (pre-BötC) [0.02]
Ramp-I (rVRG) ^a	Drive (Pons) [5]; Aug-E (BötC) [−0.1]; Early-I (2) (rVRG) [−0.3]; Post-I (BötC) [−2]; Pre-I/I (pre-BötC) [0.06]*
IE (pons) ^b	Post-I (BötC) [0.35]; Ramp-I (rVRG) [0.2]
RVLM ^b	Drive (VLM) [1]*; IE (pons) [0.05]; Post-I (BötC) [−0.05]; Post-I (e) (BötC) [0.075]*; Pre-I/I (pre-BötC) [−0.01]*

The core respiratory circuitry (^a) was adapted from Barnett et al. (2018) and the presympathetic circuitry (^b) was adapted from Baekey et al. (2010). *Weights differ from or are absent in Barnett et al. (2018) or Baekey et al. (2010).

patterns (Mandel and Schreihöfer, 2006). We identified CVLM neurons that fire in phase to inspiration as a candidate to convey inspiratory phase inhibition to the RVLM. In our model, the sole input to this CVLM population is the pre-I/I population of the pre-Bötzinger complex, such that CVLM neurons firing frequency is controlled by the pre-I/I neurons. The activity of the CVLM is used here to shape the inspiratory modulation of the RVLM and hence contribute to the inspiratory modulation of the sympathetic motor output. We present this projection from Pre-I/I neurons of the pre-Bötzinger complex to inspiratory-phase neurons of the CVLM and then subsequent inhibition of the RVLM as a hypothetical mechanism to shape inspiratory activity in the sympathetic nerve output. We model CIH induced plasticity in female rats as a persistent change to the conductance of the persistent sodium current found in the pre-I/I population; it is reduced to 25% of its value in simulations of non-CIH conditions (from 4 nS in the non-CIH simulation to 1 nS in the CIH-female simulation). This adjustment alters the firing pattern of the Pre-I/I population such that its inspiratory burst is of lesser amplitude and no longer adapting (Fig. 13).

The pattern-forming Post-I (e) population of the Bötzinger complex has been adjusted such that it fires a burst strictly on rebound from inspiratory inhibition. This was accomplished by changing its input to strong inspiratory-phase inhibition (Table 1), and by altering the kinetics of the hyperpolarization-activated current to promote rebounding activity. The hyperpolarization-activated current took the form $I_h = \bar{g}_h m_h [V - E_h]$. Its maximal conductance (\bar{g}_h) was 3 nS, and its reversal potential (E_h) was -20 mV. The activation variable (m_h) was described by its derivative: $dm_h/dt = [f(V) - m_h]/\tau(V)$. The steady state voltage dependence of this neuron's activation was $f(V) = [1 + \exp([V + 70]/5.5)]^{-1}$, and the time constant for activation was $\tau(V) = 1500 / \cosh([V + 80]/13)$ ms.

RESULTS

Increased sympathetic responses to peripheral chemoreflex activation in CIH-female rats

CIH-female rats developed changes in the respiratory pattern marked by a reduction in the inspiratory duration, T_{INSP} (Fig. 1, Panel A). Moreover, simultaneous recordings of tSNA and PN showed that CIH-female rats presented an increased average of tSNA during inspiration when compared to control as previously described by Souza et al. (2016) (Fig. 1, Panel A). Peripheral chemoreflex activation induced by KCN produced an increase in tSNA and the respiratory rate (F_R) in control and CIH rats, but the percentage of increase in tSNA in relation to the baseline average activity following peripheral chemoreflex stimulation was significantly higher in CIH-female (116.2 ± 24 vs $78.4 \pm 27\%$ of increase in tSNA, $P = 0.0103$, Fig. 1, Panel C) than in control rats. CIH-female rats ($n = 8$) presented similar F_R responses following peripheral chemoreflex activation (145.4 ± 52 vs $176.4 \pm 108\%$ of increase in F_R , $P = 0.4780$, Fig. 1, Panel D) to control ($n = 8$).

The effect of carotid body ablation on the respiratory–sympathetic coupling in CIH-female rats

Waveform averages of tSNA and PN indicate that CIH-female rats ($n = 8$) presented a reduced time of inspiration (0.71 ± 0.11 vs 1.29 ± 0.32 s, $P < 0.000$, Fig. 2, Panel A and Fig. 3, Panel A) when compared to control rats ($n = 8$) as previously described by Souza et al. (2016). In addition, no significant differences were observed in the duration of expiration, T_{EXP} (3.9 ± 1 vs 4.7 ± 2 s, $P > 0.999$, Fig. 3, Panel B) or in F_R (0.18 ± 0.04 vs 0.17 ± 0.05 Hz, $P > 0.999$, Fig. 3, Panel C) in CIH and control rats. No changes of the PN amplitude were observed between CIH-female rats and control (3.3 ± 1 vs 2.9 ± 2 μ V), Ac-CBx-CIH and Ac-CBx-Control (2.6 ± 1 vs 2.1 ± 1 μ V) or CBx-Control and CBx-CIH (2.7 ± 1 vs 2.8 ± 1 μ V). Two-way ANOVA for these variables showed no significant interaction ($p = 0.7725$) between groups. These data indicate that CIH and/or CBx do not have effect on PN amplitude in WHBP of female rats.

CIH-female rats also presented a significant increase in the average tSNA during inspiration (60.3 ± 15 vs $38.2 \pm 8\%$ of tSNA, $P = 0.0006$, Fig. 2, Panel A and Fig. 3 Panel D) when compared to control rats. There are no significant changes in average tSNA in post-inspiratory, E-1 (32.5 ± 8 vs $36.7 \pm 9\%$ of tSNA, $P > 0.999$, Fig. 3, Panel E) and late-expiratory, E-2 phases (32.5 ± 7 vs $31.3 \pm 7\%$ of tSNA, $P > 0.999$, Fig. 3, Panel F).

Acute removal of CBs after CIH conditioning (Ac-CBx) (Fig. 2, Panel B) did not abolish the increased tSNA during inspiration in CIH-female ($n = 7$) rats (68.2 ± 11 vs $42.9 \pm 10\%$ of tSNA, $P = 0.0003$, Fig. 3, Panel D) when compared to Ac-CBx-control ($n = 7$). However, Ac-CBx attenuated the reduction in T_{INSP} induced by CIH in female rat since T_{INSP} was not different between Ac-CBx-control rats (0.98 ± 0.15 vs 1.21 ± 0.2 s, $P = 0.1143$, Fig. 3, Panel A) and was significantly longer when compared to Sham CIH-female rats (0.98 ± 0.15 vs 0.71 ± 0.11 , $P = 0.0408$, Fig. 3, Panel A). No significant differences were observed after in Ac-CBx rats in the average tSNA during E-1 (43.1 ± 11 vs $43.2 \pm 12\%$ of tSNA, $P > 0.999$, Fig. 3, Panel E) or during E-2 phases (32.8 ± 9 vs $32.7 \pm 7\%$ of tSNA, $P = 0.6345$, Fig. 3, Panel F). No significant differences were observed in T_{EXP} (4.8 ± 2 vs 3.7 ± 2 s, $P = 0.5859$, Fig. 3, Panel B) or in F_R (0.17 ± 0.06 vs 0.17 ± 0.05 Hz, $P > 0.999$, Fig. 3, Panel C) in Ac-CBx-CIH and control rats. These results suggest that tonic activity of CBs contributes to changes in T_{INSP} after CIH, but plays no role in the enhanced inspiratory modulation of tSNA in CIH-female rats.

Panel C of Fig. 2 is showing the effect of CBs ablation in the respiratory–sympathetic coupling of female rats before the onset of CIH (CBx-CIH). CBx-CIH rats presented no significant differences in the average tSNA during inspiration (36.2 ± 9 vs $37.7 \pm 7\%$ of tSNA, $P > 0.999$, Fig. 3, Panel D) when compared to CBx-control ($n = 7$). Moreover, panel D of Fig. 3 shows that CBx-CIH presented a reduction on the average tSNA during inspiration when compared to Sham CIH-rats (36.2 ± 9 vs $60.3 \pm 15\%$ of tSNA, $P = 0.0003$) suggesting that CB integrity during conditioning is

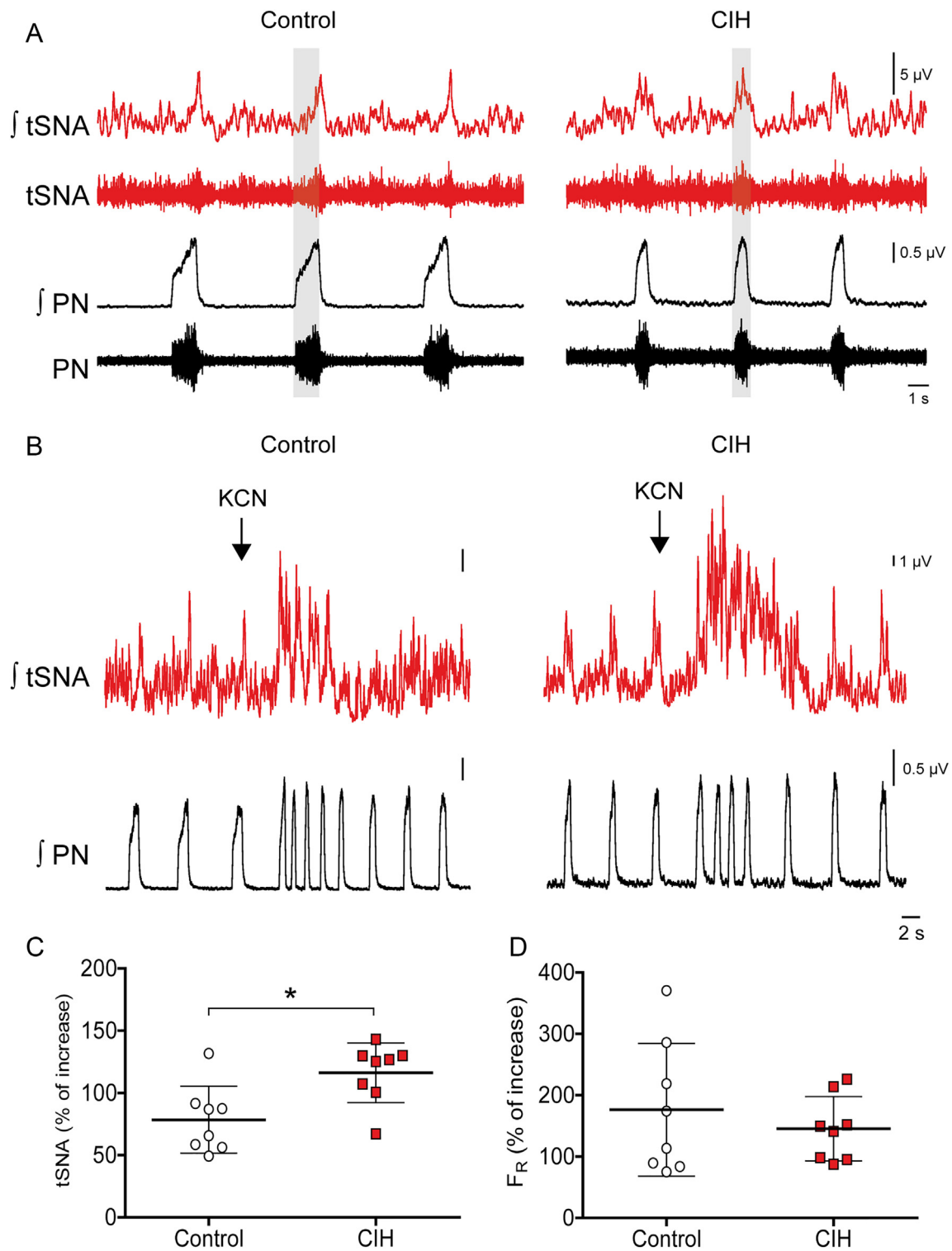


Fig. 1. Changes in respiratory–sympathetic coupling and in sympathetic response to peripheral chemoreflex activation in CIH-female rats. (A) Baseline recordings of thoracic sympathetic nerve (tSNA) and phrenic nerve (PN) activities of a female rat representative from control (left) and CIH group (right) showing the increase in average tSNA during inspiration in CIH-female rats in relation to the tSNA peak (100%) and the electrical noise (zero). (B) Sympathetic and respiratory response to peripheral chemoreflex activation with KCN in a CIH-female rat and control. Note that average amplitude of tSNA in relation to baseline is enhanced in CIH-female rats compared to control after KCN. (C) Average and individual values of the percentage of increase in average tSNA related to the average baseline activity after KCN in CIH (n = 8) and control (n = 8) female rats. (D) Average and individual values of the percentage of increase in respiratory frequency related to baseline after KCN in CIH and control female rats. * P < 0.05.

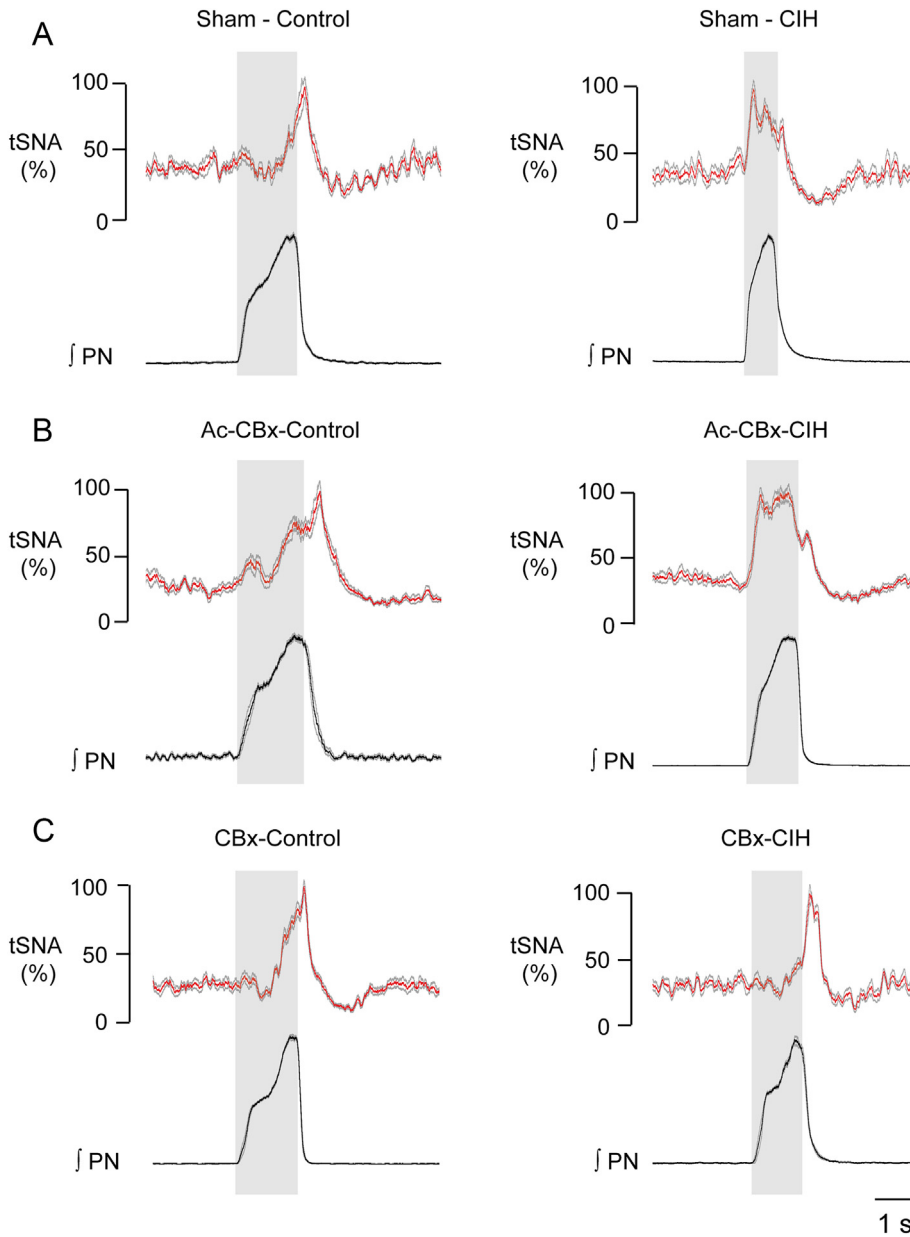


Fig. 2. The effect of carotid body ablation on the respiratory sympathetic coupling of CIH-female rats. (A) Waveform averages of thoracic sympathetic activity (tSNA) and phrenic nerve (PN) of a control and a CIH female rat representative from the Sham surgery group. The peak of integrated tSNA during the respiratory cycle was considered 100% of activity and the electrical noise, zero. Note that CIH-female rats presented an increase in the average tSNA during the inspiration when compared to control rats. (B) Waveform averages of tSNA and PN of a control and a CIH female rat representative from the acute surgical removal of carotid bodies (after CIH protocol, Ac-CBx) group. Note that Ac-CBx does not affect the enhanced inspiratory modulation of tSNA after CIH in female rats. However, Ac-CBx prevented the reduction on the time of inspiration (T_{INSP}) in CIH rats. (C) Waveform averages of tSNA and PN of a control and a CIH female rat representative from the surgical removal of carotid bodies (CBx) before the onset of CIH protocol. Note that in this case, CBx prevented the increase in the inspiratory modulation of tSNA after CIH in female rats as well as the reduction in T_{INSP} .

important to drive the increase in the inspiratory modulation of tSNA in CIH female rats. No significant differences were observed in the average tSNA during E-1 (39.6 ± 9 vs $33.9 \pm 11\%$ of tSNA, $P = 0.8579$, Fig. 3, Panel E) or during E-2 (31.8 ± 13 vs $28.4 \pm 10\%$ of tSNA, $P > 0.999$, Fig. 3, Panel F) of CBx-CIH female rats compared to CBx-control female rats. Additionally, chronic CBx prevented the

reduction in T_{INSP} in CIH-female rats because T_{INSP} was not different from chronic CBx-control (1.13 ± 0.14 vs 1.05 ± 0.18 s, $P > 0.999$) and was significantly longer than in Sham CIH-rats (1.13 ± 0.14 vs 0.71 ± 0.11 , $P = 0.0008$, Fig. 3, Panel A). No significant differences were observed in T_{EXP} (3.9 ± 1 vs 3.8 ± 0.7 s, $P > 0.999$, Fig. 3, Panel B) or in F_R (0.16 ± 0.03 vs 0.16 ± 0.01 Hz, $P > 0.999$, Fig. 3, Panel C) in CBx-CIH and control rats. Taken together, these results indicate that CBs activation during CIH is essential to promote the increase in the average tSNA during the inspiratory phase of respiratory cycle in CIH-female rats.

Increase in sEPSCs frequency in the NTS neurons of CIH-female rats

We recorded sEPSCs from NTS neurons of female rats to test the hypothesis that CIH induces an increase in excitatory neurotransmission at this region (Fig. 4, Panels A and B), which might contribute to the observed changes in the sympathetic–respiratory coupling and to the enhanced peripheral chemoreflex response. NTS neurons from CIH-female rats ($n = 7$) presented an increase in sEPSC frequency (3.12 ± 2.4 vs 0.75 ± 0.3 Hz, $P = 0.0414$, Fig. 4, Panel C) when compared to NTS neurons from controls ($n = 6$). However, the amplitude of sEPSC (23.6 ± 8 vs 18.9 ± 4 pA; $P = 0.2558$, Fig. 4, Panel D) was not different between NTS neurons from CIH-female rats compared to control. No differences were observed in the half-width of sEPSCs either (3.2 ± 0.6 vs 3.1 ± 1 ; $P = 0.8054$, Fig. 4, Panel E). This indicates that the spontaneous excitatory neurotransmission activity in NTS is increased in CIH-female rats compared to control in medullary slices (*i.e.* in absence of CBs).

Firing properties of inspiratory neurons after CIH in female rats

Pre-I/I neurons ($n = 17$) of CIH-female rats presented a significant reduction of the mean firing frequency (47.3 ± 34 vs 107.6 ± 58 Hz, $P = 0.0018$) when compared to neurons

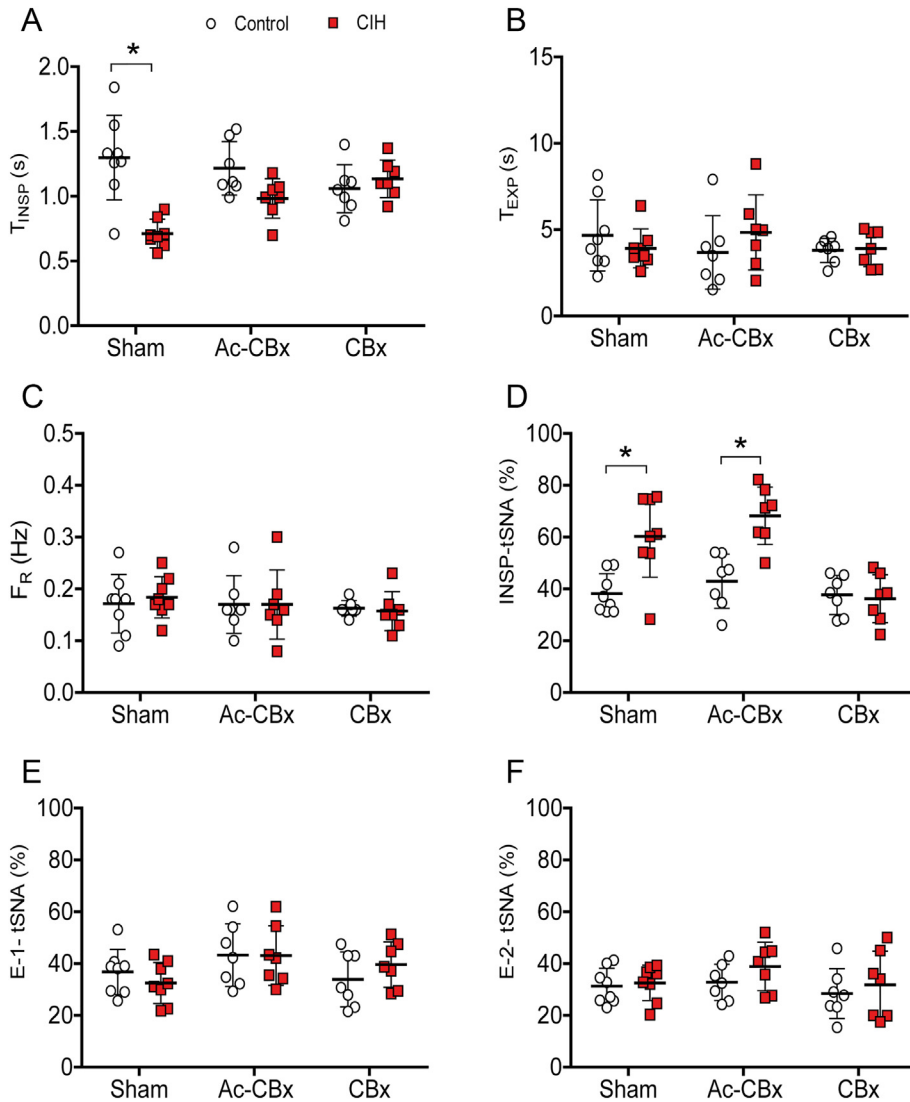


Fig. 3. Average and individual values of time of inspiration (T_{INSP} , A), time of expiration (T_{EXP} , B), respiratory frequency (F_R , C), average thoracic sympathetic activity (tSNA) during the inspiratory (D), early expiratory (E) and late-expiratory (F) phases of the respiratory cycle of Sham-control ($n = 8$), Sham-CIH ($n = 8$), Ac-CBx-control ($n = 7$), Ac-CBx-CIH ($n = 7$), CBx-control ($n = 7$) and CBx-CIH ($n = 7$). Values are mean \pm SD. * $P < 0.05$. The values of tSNA were obtained from the integrated tSNA signal and are expressed as percentage in relation to the peak tSNA during the respiratory cycle (100%) and the electrical noise (zero).

from control rats ($n = 15$, Fig. 5). Firing frequency was also reduced in Pre-I/I of CIH rats during inspiration (70.1 ± 37 vs 126.6 ± 55 Hz, $P = 0.0018$) compared to control, but not in the pre-inspiratory period (20.9 ± 11 vs 29.9 ± 18 Hz, $P = 0.0541$). The relative duration of pre-inspiratory activity of Pre-I/I neurons from CIH-female rats (30.7 ± 26.4 vs $34.4 \pm 23\%$ of T_{EXP}) was also not different in relation to control rats (Fig. 5, Panel E). These data indicate that CIH induces a reduction of Pre-I/I neuron firing rate during the inspiratory period in CIH-female rats.

Early-I neurons ($n = 7$) from CIH female rats presented no significant changes in the firing frequency (48.6 ± 20 vs 38.9 ± 16 Hz, $P = 0.3384$) when compared to neurons from control animals ($n = 10$, Fig. 6). Their relative firing time $T_{\text{EARLY-I}}$ was not significantly different between CIH (85.0 ± 12 vs $84.2 \pm 13\%$ of T_{INSP} , $P = 0.9108$) and control female

rats. Fig. 7 show that Late-I neurons from CIH female rats ($n = 11$) presented no significant changes in the firing frequency (21.5 ± 13 vs 15.8 ± 12 Hz, $P = 0.3238$) when compared to neurons from control animals ($n = 9$). The $T_{\text{LATE-I}}$ was not significantly different between CIH (36.9 ± 17 vs $26.4 \pm 16\%$ of T_{INSP} , $P = 0.1770$) and control female rats. Ramp-I neurons from CIH female rats ($n = 14$) also presented no significant changes in the firing frequency (85.1 ± 54 vs 69.8 ± 33 Hz, $P = 0.7340$) when compared to neurons of control animals ($n = 14$, Fig. 8).

Firing properties of expiratory neurons after CIH in female rats

Post-I neurons from CIH female rats ($n = 15$) presented no changes in the mean firing frequency (32.1 ± 15 vs 31.4 ± 17 Hz, $P = 0.7915$) when compared to Post-I neurons from control rats ($n = 17$, Fig. 9). However, the time of their activity was increased in CIH-female rats (92.3 ± 7 vs $81.4 \pm 12\%$ of T_{EXP} , $P = 0.0127$, Fig. 9, Panel B) compared to control, indicating that Post-I neurons fire for a longer time during the expiration in CIH-female rats. Fig. 10 shows that Aug-E neurons from CIH-female rats ($n = 12$) presented no significant changes in the firing frequency (40.8 ± 29 vs 47.4 ± 24 Hz, $P = 0.5357$) when compared to Aug-E neurons from control female rats ($n = 13$). The period of their activity (33 ± 20 vs $42.6 \pm 16\%$ of T_{EXP} , $P = 0.2381$) was also not significantly different between CIH and control rats respectively (Fig. 10, Panel C). As illustrated in Fig. 11, Late-E neurons were silent in CIH-female rats in normocapnic conditions of WHBP ($\text{CO}_2 = 5\%$). However, their activity could be induced ($n = 3$) by hypercapnia ($\text{CO}_2 = 10\%$).

Simulations of CIH in female rats

We reproduced the effects of CIH conditioning of female rats in our computational model of brainstem respiratory and pre-sympathetic circuitry. The goal of these simulations was to hypothesize on theoretical mechanisms that explained the difference in sympathetic output – the increase in activity due to loss of ramping pattern in SNA from CIH conditioned female rats (Souza et al., 2016) – in

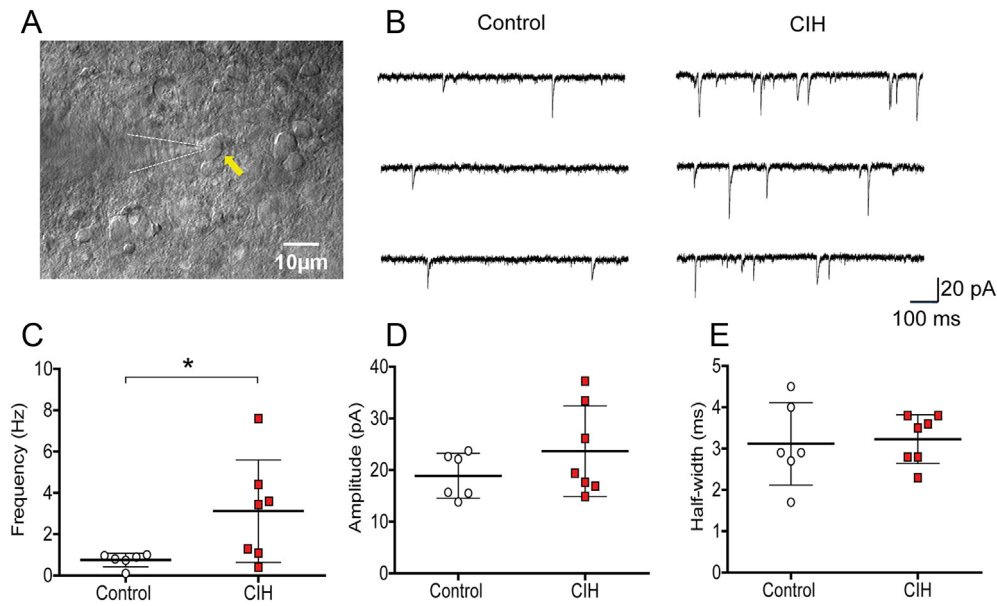


Fig. 4. Spontaneous excitatory neurotransmission within NTS in CIH and control female rats. (A) Photomicrography of a medullary slice of one representative rat showing a single NTS neuron and the recording electrode. (B) Recordings of spontaneous excitatory post-synaptic currents (sEPSC) from an NTS neuron from control (left) and of CIH (right). Note the increase in the frequency of sEPSC in the NTS neuron of a CIH-female rat. (C) Average and individual values of the sEPSC frequency in NTS neurons from CIH ($n = 7$) and control ($n = 6$) rats. (D) Average and individual values of the sEPSC amplitude in NTS neurons from CIH and control rats. (E) Average and individual values of the sEPSC half-width in NTS neurons from CIH and control rats. * $P < 0.05$.

a way that can associate it with the differences observed in neuronal firing pattern between non-CIH and CIH-conditioned female rats. Specifically, *via* model simulations, we test the plausibility of the following hypotheses: (1) the ramping inspiratory component of the sympathetic output is shaped by decrementing inhibition; and (2) CIH conditioning induces a persistent change that reduces this inhibition and thus increases the sympathetic output during inspiration. In the model, we incorporate mechanisms that establish causal relationship between the facts that pre-I/I neurons have a lower inspiratory firing rate (Fig. 5) and that sympathetic activity loses the ramping pattern (Fig. 2A, B) and overall increases during inspiration (Fig. 3D) in CIH conditioned female rats.

It has been suggested that excitatory neurons of the pre-Bötzinger complex possess slowly inactivating persistent sodium current (I_{NaP}) whose inactivation occurs on a time-scale of seconds (Butera et al., 1999; Rybak et al., 2014; Jasinski et al., 2013). We implement these excitatory neurons in our computational model as excitatory Pre-I/I neurons of the pre-Bötzinger complex (Smith et al., 2007). The slow inactivation of I_{NaP} results in a decrementing pattern of activity in these neurons during inspiration. We hypothesize and implement in the model that a decrementing firing pattern of pre-I/I neurons correspondingly shapes the inspiratory-phase sympathetic activity. In this model, the pre-I/I population provides the main input to an inhibitory CVLM population. In turn, the CVLM neurons provide inhibition to the RVLM (Schreihofer and Guyenet, 2002), and also exhibit respiratory-modulated firing pattern (Mandel and Schreihofer, 2006). Thus, in our model the CVLM population

receives decrementing excitation from pre-I/I and, therefore, provides decrementing inhibition to the RVLM in control simulations. Its pattern of activity is subject to modulation of pre-Bötzinger complex pre-I/I neurons such that a reduction in their firing rate and a change in their firing pattern are translated to a change in the strength and shape of inhibition onto RVLM (Fig. 12). In simulations, we show that the above mechanisms closely reproduce the transformation of the shape of the sympathetic output from a ramping pattern to a “blocky” pattern and overall increase in sympathetic activity during inspiration as observed following CIH conditioning in female rats.

Pre-Bötzinger pacemaker neurons may shape the inspiratory component of SNA

In simulations of non-CIH conditions, the Pre-I/I population fires a rebound burst following the removal of expiratory inhibition. Strong inhibition during expiration removes the inactivation of I_{NaP} such that this current is strongest at the beginning of the inspiratory burst. Over the duration of this burst, I_{NaP} slowly inactivates, and the firing rate of the population decrements (Fig. 13). This pattern of activity is transmitted to CVLM such that it fires an inspiratory burst with the same shape. Therefore, RVLM receives relatively strong inhibition from CVLM at the beginning of inspiration and relatively weak inhibition at the end of inspiration; in this way the sympathetic output is made to have a ramping shape (Fig. 14).

I_{NaP} is subject to enhancement during hypoxia (Hammarstrom and Gage, 2002; Paton et al., 2006). Hence, it is likely that pacemaker neurons of the pre-Bötzinger complex are over-excited during hypoxic episodes of CIH conditioning due to enhancement of I_{NaP} . We suggest that in CIH conditioned female rats, this over-excitation induces a compensatory activity-dependent mechanism such that pacemaker neurons are less excitable during normoxia compared to those in non-CIH female rats. In our computational model, this plasticity is implemented as a substantial reduction of the conductance of I_{NaP} . This change in excitability abolishes the decrementing pattern of activity in Pre-I/I activity during inspiration (Fig. 13) without disrupting the three-phase respiratory rhythm.

In CIH simulations, the firing rate of pre-I/I is reduced and does not change substantially over the course of inspiration

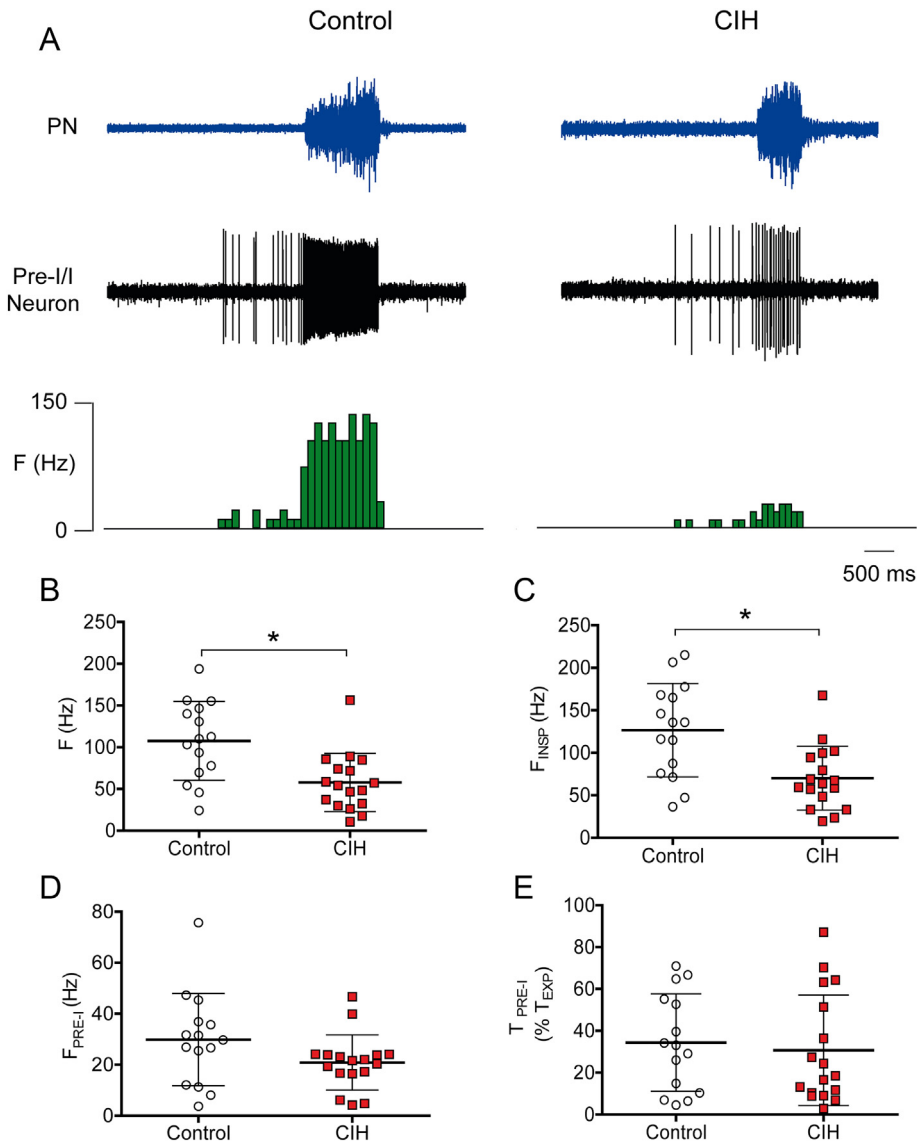


Fig. 5. Pre-inspiratory/inspiratory (Pre-I/I) neuron activity in CIH-female rats. (A) Recordings of Pre-I/I neurons representative from control and CIH-female rats. Note that Pre-I/I neurons from CIH-female rats presented a reduction in firing frequency when compared to control. Average and individual values from CIH ($n = 17$) and control ($n = 15$) group of Pre-I/I total firing frequency (B), frequency during inspiration (C), during the pre-inspiratory phase (D) and the duration of the pre-inspiratory phase activity (E). Bin size = 100 ms. Values are mean \pm SD. * $P < 0.05$.

(Fig. 13), and this pattern is transmitted to the CVLM population (Fig. 14). As such, the RVLM population is disinhibited at the beginning of the inspiratory phase compared to the non-CIH simulation, and its firing rate does not change substantially over the course of inspiration (Fig. 14). In this way, the reduction of firing rate of the Pre-I/I population is responsible for the “blockiness” of the inspiratory-phase sympathetic burst.

CIH conditioning does not alter the expiratory activity in the sympathetic output of female rats (Souza et al., 2016). We adapted an excitatory post-inspiratory population (Post-I (e)) to account for the post-inspiratory component of the inspiratory/post-inspiratory sympathetic burst (see Methods). Previous instances of our computational model

do not address this aspect of sympathetic activity. This population fired a brief rebound burst following strong inspiratory inhibition (Fig. 14). Post-I (e) is not subject to input from Pre-I/I; since its activity is independent of Pre-I/I, this component of sympathetic output is not altered in the CIH simulation.

DISCUSSION

This study explores the effects of CIH on the firing properties of respiratory neurons in an intact ponto-medullary respiratory network in female rats exclusively. Moreover, here we reveal the critical role of CBs in the altered respiratory–sympathetic coupling induced by CIH in female rats. The aim of this study was to investigate the neural mechanisms associated with increased inspiratory modulation of SNA in CIH-female rats rather than compare the sex-related differences underlying these mechanisms. However, we used previous data from our laboratory (from experiments performed under similar conditions) to address some putative sex-differences on those neural mechanisms. The main findings of this study are the following: 1) female rats exposed to CIH develop changes in the respiratory–sympathetic coupling associated with enhanced peripheral chemoreflex; 2) carotid bodies ablation before CIH prevents the increase in SNA during inspiration in CIH-female rats; 3) Spontaneous excitatory neurotransmission at the NTS is increased in CIH-female rats; 4) Pre-I/I neurons have

reduced their firing frequency in female rats exposed to CIH; 5) Post-I neurons have increased time of firing in CIH-female rats. All together, these observations indicate that intermittent activation of peripheral chemoreceptors in female rats during CIH contributes to changes in the respiratory–sympathetic network activities that drive sympathetic overactivation during inspiration in these rats.

Enhanced SNA responses to peripheral chemoreflex activation in CIH-female rats

Sympathetic responses to peripheral chemoreflex stimulation are increased in spontaneously hypertensive rats (SHR) (Pijacka et al., 2016b), in two-kidney, one-clip hypertensive rats (Oliveira-Sales et al., 2016) and in CIH-male rats (Braga et al., 2006) and in sustained hypoxia (Accorsi-

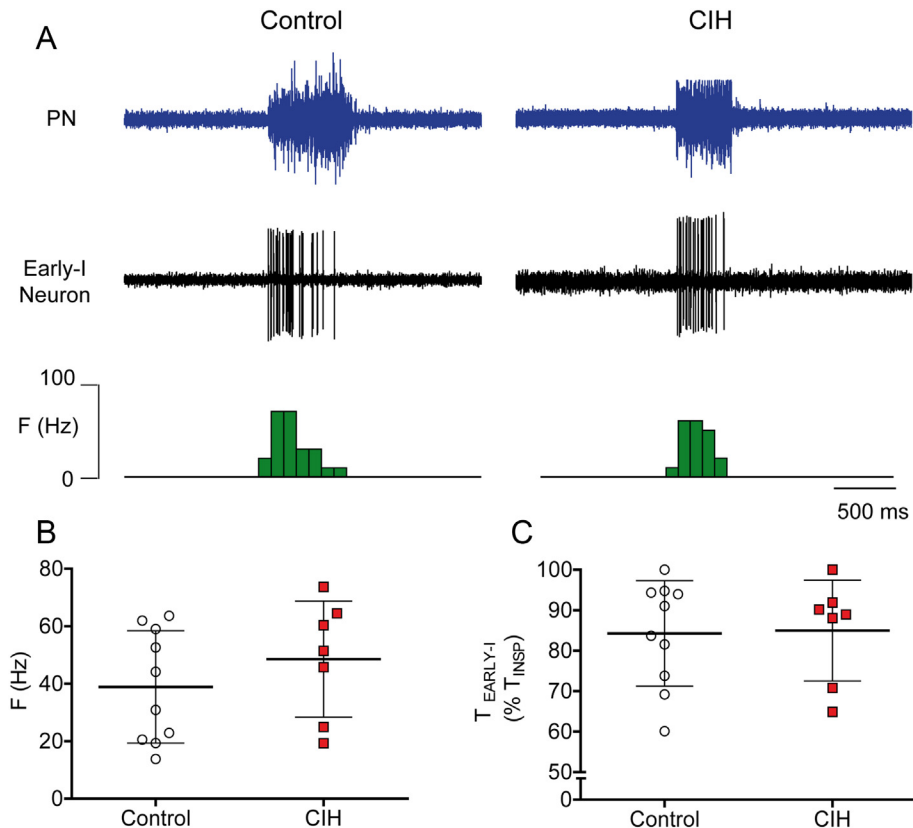


Fig. 6. Early-inspiratory neurons (Early-I) activity in CIH-female rats. (A) Recordings of Early-I neurons representative from control and CIH-female rats. Average and individual values from CIH ($n = 7$) and control ($n = 10$) group of Early-I neurons firing frequencies (B) and the duration of activity relative to the duration of inspiratory phase (C). Values are mean \pm SD. Bin size = 100 ms.

Mendonca et al., 2015) suggesting that this reflex is sensitized in these experimental models of hypertension. Given that peripheral chemoreflex stimulation increases the activity of pre-sympathetic and respiratory neurons, the enhancement in peripheral chemoreceptors sensitivity seems to produce an amplification in the respiratory–sympathetic coupling in SHR (McBryde et al., 2013). Female rats exposed to CIH develop hypertension and sympathetic overactivity (Souza et al., 2015, 2016, 2017). Previous and present studies documented that CIH-female rats exhibited changes in respiratory–sympathetic coupling marked by an increase in the inspiratory modulation of sympathetic activity (Souza et al., 2016). Additionally, we are documenting that CIH-female rats also present an enhanced SNA response following peripheral chemoreflex activation compared to control rats, similarly to other models of hypertension.

The exaggerated SNA response to peripheral chemoreflex activation in rats exposed to CIH seems to be related to the increase in the sensitivity of glomus cells of CBs in response to hypoxia as well as to a possible increase in excitatory neurotransmission at the level of brainstem respiratory and autonomic neurons (Iturriaga et al., 2009; Costa-Silva et al., 2012; Del Rio et al., 2014). In fact, direct recordings of CBs afferent activity show that glomus cells of CIH-male rats are more sensitized to acute hypoxia (Del Rio et al., 2010, 2014; Nanduri et al., 2017). Studies by Costa-Silva et al. (2012) using the WHBP of

rats documented that glutamatergic neurotransmission is augmented in the NTS of CIH-male rats. This statement is supported by the fact that CIH-male rats had an increase in the expression of ionotropic glutamate receptors at NTS and the SNA response to microinjection of L-glutamate into the same region was significantly greater in CIH-male rats compared to control (Costa-Silva et al., 2012). Taken together, these findings suggest that the enhanced glutamatergic signaling at the NTS contributes to the exaggerated SNA response to peripheral chemoreflex activation in CIH-male rats (Costa-Silva et al., 2012).

Here we evaluated the synaptic transmission aspect at the NTS using the whole cell patch-clamp technique to record the sEPSCs in CIH-female rats. The isolated sEPSCs are an index of excitatory neurotransmission at the NTS (Accorsi-Mendonca et al., 2015). Electrophysiological recordings showed that the frequency of sEPSCs is increased in NTS neurons of CIH-female when compared to NTS neurons from control rats. These data suggest that CIH induces an increase in the spontaneous glutamatergic transmission at NTS neurons

which is likely to contribute to the overall enhanced excitability of the peripheral chemoreflex pathway in CIH-female rats. Additionally, this suggests that increased excitatory neurotransmission in NTS is related to presynaptic mechanisms since the effect of CIH was restricted to the frequency of spontaneous currents and not to their amplitude or half-width. The increase in sEPSCs frequency seems to be related to an increase in the probability of spontaneous neurotransmitter release or in the number of synapses or synaptic active zones on the presynaptic terminal (Stevens and Wang, 1994). It is likely that the intermittent activation of these synaptic terminals by CBs afferents induces this facilitation of neurotransmitter release in CIH-female rats. This phenomenon also could be important to produce sustained SNA increase after the acute removal of CBs in CIH-female rats (Fig. 2, Panel B), as discussed below. However, further experiments are necessary to identify the mechanisms of CIH effect on the presynaptic terminals in the NTS in female rats.

Changes in respiratory–sympathetic coupling of female rats exposed to CIH are dependent on carotid bodies integrity

Under baseline conditions, glomus cells at CBs have little or no activity (Prabhakar and Semenza, 2015). However, evidences indicate that abnormal activity of these oxygen

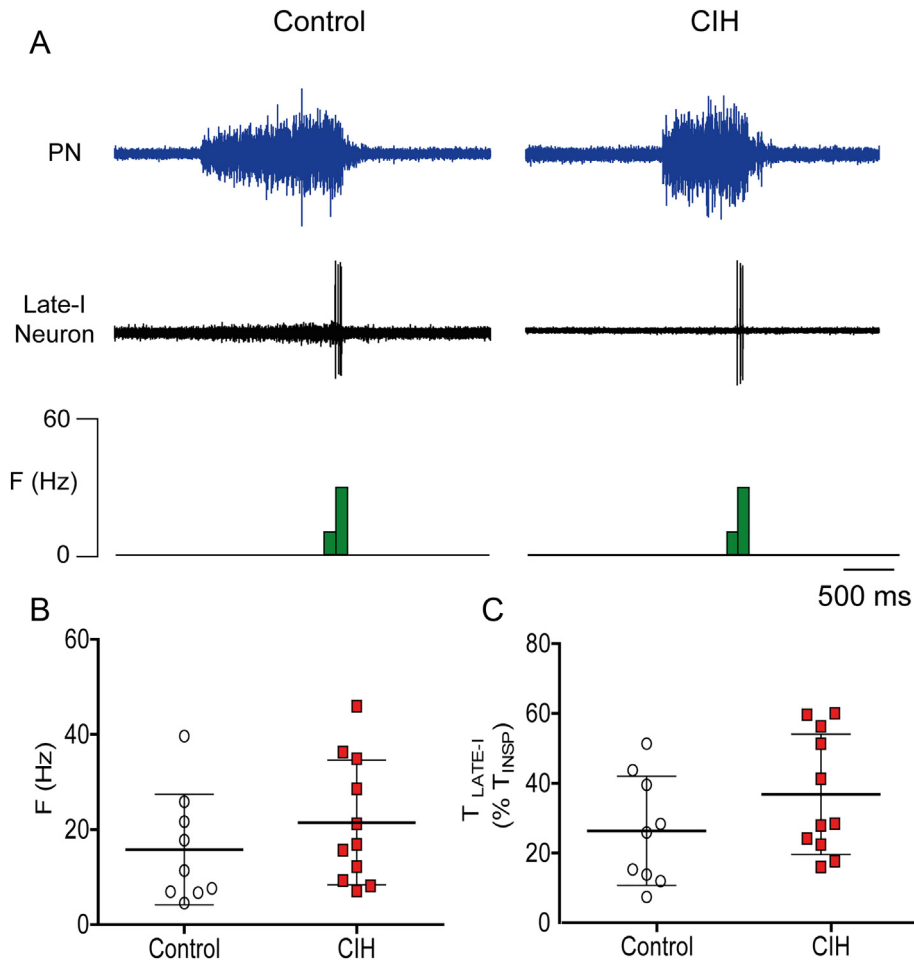


Fig. 7. Late-inspiratory neurons (Late-I) activity in CIH-female rats. (A) Recordings of Late-I neurons representative from control and CIH-female rats. Average and individual values from CIH ($n = 11$) and control ($n = 9$) group of Late-I neurons firing frequencies (B) and the duration of activity relative to the duration of inspiratory phase (C). Values are mean \pm SD. Bin size = 100 ms.

sensors could contribute to the development of sustained sympathetic overactivity leading to hypertension in humans (Narkiewicz et al., 2016; Pijacka et al., 2016b) and in experimental models (Abdala et al., 2012; McBryde et al., 2013; Del Rio et al., 2016; Pijacka et al., 2016a). In fact, surgical removal of CBs reduces arterial blood pressure in drug-resistant hypertensive subjects (Narkiewicz et al., 2016). In OSA patients, it has been demonstrated that acute CBs silencing with hyperoxia ($O_2 = 100\%$) reduces MSNA in those patients but not in control or normotensive subjects (Narkiewicz et al., 1998b). This latter study indicates that tonic activity of CBs plays an important role in the enhancement of MSNA in OSA patients (Narkiewicz et al., 1998b).

Increased tonic activity of CBs has been hypothesized as one of the causative factors producing amplified respiratory-sympathetic coupling and to sympathetic overactivity in male SHR (McBryde et al., 2013). This hypothesis is supported by the fact that acute CBs ablation reduces the respiratory modulation of sympathetic activity in SHR (McBryde et al., 2013). In the experimental model of CIH, acute removal of CBs in male rats produced no effect on the enhanced respiratory modulation of sympathetic activity

(Zoccal et al., 2008). However, removal of CBs before the beginning of CIH protocol prevented the enhanced respiratory modulation of SNA in CIH-male rats (Moraes and Machado, 2015). Taken together, these evidences show that in CIH-male rats, CBs play an important role in inducing changes in respiratory-sympathetic coupling during the time course of CIH but exert no major role in the maintenance of these changes in respiratory-sympathetic coupling (Zoccal et al., 2008; Moraes and Machado, 2015).

In this study we hypothesized that CBs integrity is essential to induce changes in the respiratory-sympathetic coupling in CIH-female rats during the time course of CIH protocol. In female rats exposed to CIH, acute removal of CBs produced no changes in the enhanced inspiratory modulation of sympathetic activity; however, it reversed the reduction of inspiratory time induced by CIH. This observation indicates that, different from CIH-male rats, tonic activity of CBs is important to drive certain changes in the respiratory activity of CIH-female rats. We speculate that these sex differences observed in CBs tonic activity after CIH may be related to sexual dimorphism in the CBs activity or in the neural structures involved in the peripheral chemoreflex pathways, such as the pre-BötC neurons (Garcia et al., 2013).

Importantly, with acute removal of CBs we were able to dissociate the changes of respiratory pattern and sympathetic overactivity in CIH-female rats. These results indicate that separate mechanisms support the reduction in T_{INSP} and the increased modulation of SNA during the inspiratory phase, for example plastic changes in respiratory neurons induced during the time course of CIH (discussed below). Considering that the excitatory neurotransmission at NTS is increased in brainstem slices (*i.e.*, in the absence of CBs) of CIH-female rats, we suggest that this phenomenon could also contribute to enhanced SNA during inspiration even after the acute CBs removal.

Changes in the inspiratory neurons firing frequency after CIH in female rats

Taking into consideration that CIH-female rats develop changes in the pattern of SNA during the inspiratory phase, in this study we aimed to verify whether or not the inspiratory neurons present changes in their firing properties in CIH-female rats. We are showing that Pre-I/I respiratory neuron type has reduced the firing frequency after CIH and there is evidence that these neurons possess the persistent sodium current

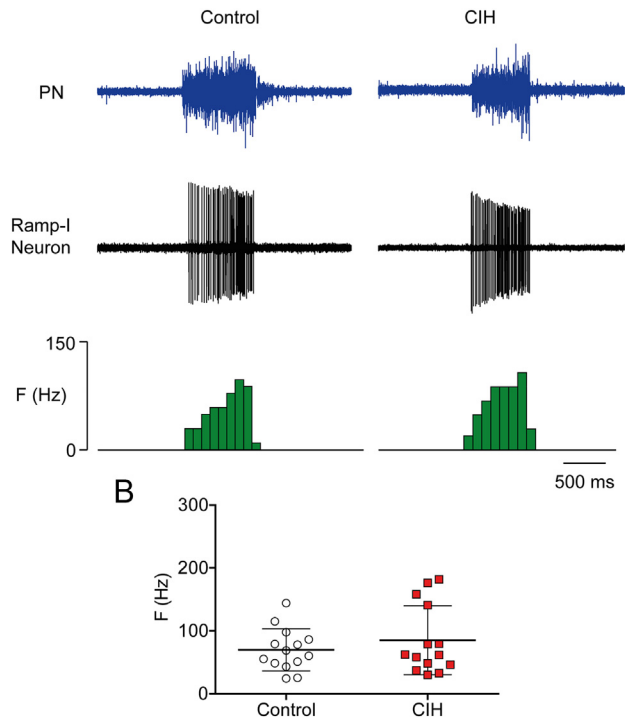


Fig. 8. Ramp-inspiratory neurons (Ramp-I) activity in CIH-female rats. (A) Recordings of Ramp-I neurons representative from control and CIH-female rats. Average and individual values from CIH ($n = 14$) and control ($n = 14$) group of Ramp-I neurons firing frequencies (B). Values are mean \pm SD. Bin size = 100 ms.

(I_{NaP}), which is likely to contribute to their pacemaker activity (St-John and Paton, 2003; Richter and Smith, 2014). The reduced firing frequency of Pre-I/I neurons after CIH could be due to changes in their intrinsic electrophysiological properties or a product of the enhanced inhibitory inputs from the respiratory network. Here, we simulated one of the possibilities: an alteration in I_{NaP} expression in Pre-I/I neurons of CIH-female rats. The reduced I_{NaP} in Pre-I/I neurons of CIH female rats appeared sufficient to explain the reduced firing frequency and the increase in SNA during the inspiratory period.

Intracellular recordings of Pre-I/I neurons in an intact respiratory network allow the observation of changes in membrane potential of these neurons along the respiratory cycle (Moraes et al., 2014; Richter and Smith, 2014). Of note, Pre-I/I neurons present a pronounced hyperpolarization during the post-inspiratory period which gradually reduces in the time course of expiration, strongly suggesting that this inhibition is due to inhibitory post-inspiratory neurons influence (Richter and Smith, 2014). An alternative explanation for the reduced firing frequency of Pre-I/I neurons in CIH-female rats could be the increased in Post-I activity (discussed below) which may produce a prolonged inhibition of Pre-I/I neurons in CIH-female rats.

Changes in the expiratory neurons firing properties after CIH in female rats

CIH-female rats presented changes in firing properties of Post-I neurons, characterized by an increase in the time of their firing relative to the expiratory phase. Studies by

Pierrefiche et al. (1995) showed that the “spike frequency adaptation” (i.e. progressive reduction of firing frequency until the cessation of activity) of Post-I neurons is dependent on Ca^{2+} conductance. When BAPTA, a Ca^{2+} chelator, is dialyzed into the cell body of a Post-I neuron the membrane potential depolarizes and the time of firing increases (Pierrefiche et al., 1995). Studies by Moraes et al. (2014) documented similar finding in Post-I neurons of SHR, in which the increased firing frequency of Post-I neurons was driven by a reduction in Ca^{2+} -dependent K^{+} conductance, which in turn also increases the excitability of these cell type and leads to a more depolarized membrane potential during expiration (Moraes et al., 2014). A possible explanation for the observed increase in the firing time of Post-I in CIH-female rats is that CIH induces changes in the Ca^{2+} or Ca -dependent K^{+} conductance of these neurons which prolong the spike frequency adaptation process, leading to an increase in the duration of their activity. Further studies using intracellular recordings of Post-I neurons in CIH-female rats are required to test this hypothesis.

Sex differences in the respiratory neuron activity after CIH in rats

The present study describes changes in the respiratory neurons' firing properties in CIH-female rats which are different in relation to the same neurons subtypes recorded in CIH-male rats (Machado et al., 2017). In CIH-male rats, Post-I neurons presented a reduced firing frequency, an increase in the firing frequency of Aug-E neurons and rhythmic activity of Late-E neurons in resting conditions (Machado et al., 2017). This latter study suggests that the activity of expiratory neurons is altered in male rats after CIH leading to active expiration and enhanced excitatory modulation of SNA during expiration (Machado et al., 2017). In contrast, Pre-I/I neurons of CIH-female rats presented a reduction in the firing frequency, which may be related to the reduced time of inspiration. Different from those neurons in CIH-male rats, Post-I neurons presented an increase in their time of activity and Late-E neurons are not spontaneously active in normocapnia in CIH-female rats.

Sex-specific effects of CIH on the respiratory neuronal activity may be related to sex differences in the respiratory network structure and function, synaptic interactions with and within pre-BötC and in differences linked to intrinsic electrophysiological properties between female and male respiratory neurons. Experimental evidences indicated that there are sex differences in the intrinsic properties of the respiratory network in response to hypoxia which involve the activity of K_{ATP} channels in the Pre-BötC (Garcia et al., 2013). Further experiments are required to check the possible sex differences in the intrinsic characteristics of respiratory neurons in the network context as well as their intrinsic electrophysiological properties in rats exposed to CIH.

Model justification

Previously, we described how sensitization of the central chemoreflex could promote the emergence of active expiration at normocapnia and prevent apnea following the loss of

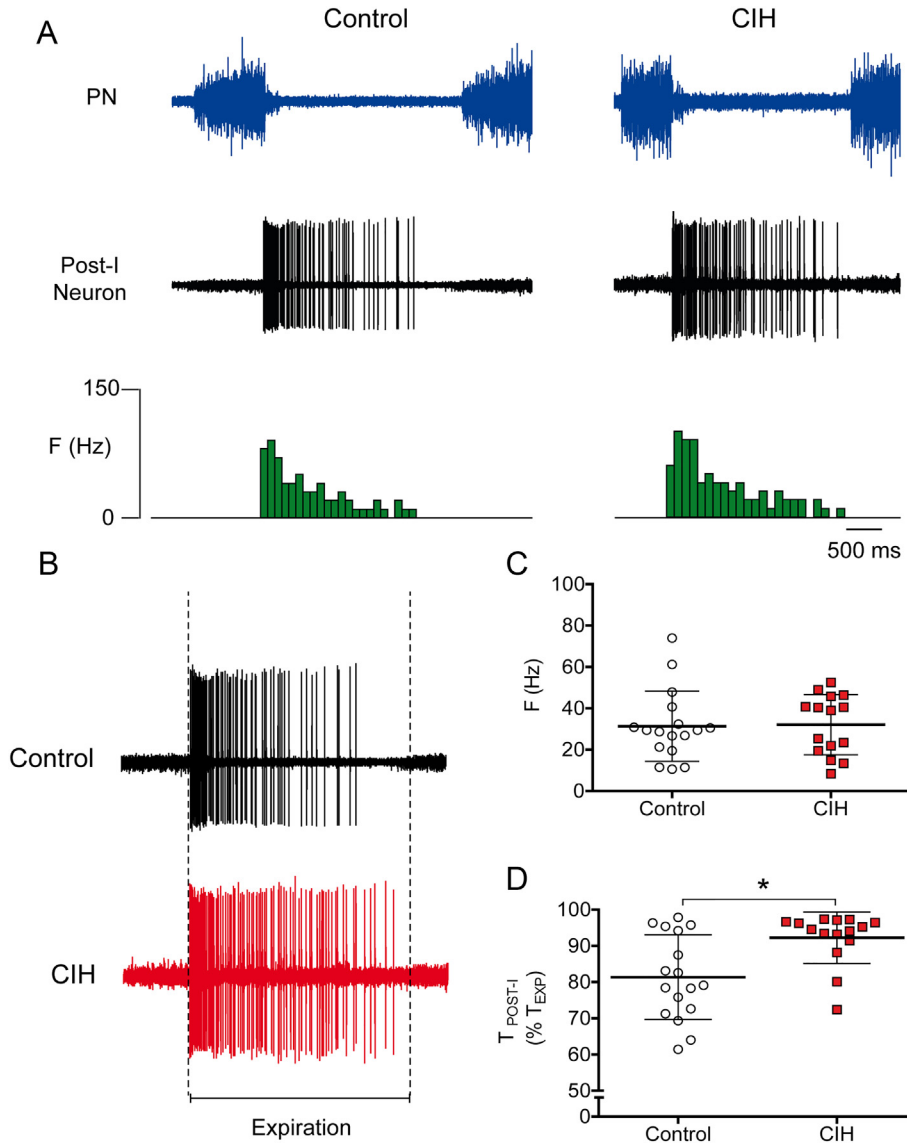


Fig. 9. Post-inspiratory (Post-I) neuron activity in CIH-female rats. (A) Recordings of Post-I neurons representative from control and CIH-female rats. (B) Representative recordings of Post-I neurons of control and CIH rats showing the increase in their firing time relative to the duration of expiratory phase. Note that Post-I neurons from CIH-female rats presented an increase in the duration of their activity relative to expiratory time. Average and individual values from CIH ($n = 15$) and control ($n = 17$) group of Post-I firing frequency (C), the duration of their activity relative to expiratory phase (D). Values are mean \pm SD. Bin size = 100 ms. * $P < 0.05$.

chemosensitive drive during hypocapnia in CIH conditioned male rats (Molkov et al., 2011). We also suggested that an increase in the excitability of pacemaker Pre-I/I neurons could be responsible for the sensitization of the central chemoreflex in CIH conditioned male rats (Barnett et al., 2017). However, these phenomena are not reported in CIH female rats. Here we utilize our computational model to develop an alternative hypothesis for CIH-induced plasticity in female rats.

The model was previously developed from data primarily drawn from male rats. However, the three phases of eupneic respiration are similarly identifiable in neuronal recordings during eupnea in both male and female rats. As such, we assert that it is acceptable to adapt the kernel of

the respiratory CPG for female experimental observations despite having been developed based on data from male rats. We take the core respiratory model of eupneic breathing as valid for eupnea in male and female rats. Then we distinguish female simulations by extending the model to account for female rat experimental data. This adapted model is informed by two critical experimental observations: (1) there is a decrease in the firing rate of pre-inspiratory/inspiratory neurons during inspiration in CIH conditioned female rats (Fig. 5) and (2) the inspiratory component of the sympathetic motor output is not ramping in CIH conditioned female rats (Souza et al., 2016). We propose that the ramping shape of the inspiratory-phase sympathetic output in non-CIH animals is formed by decrementing inspiratory-phase inhibition. Pacemaker neurons of the pre-Bötzinger complex are a good candidate for the source of this decrementing pattern due to their possessing I_{NaP} . Slow inactivation of I_{NaP} provides a mechanism for adaptation of firing rate during inspiration (Fig. 13). These pacemaker neurons appear in our computational model as the excitatory Pre-I/I population (Smith et al., 2007) (Fig. 12).

Here, we suggest that CIH conditioning induces plasticity in pacemaker neurons of the pre-Bötzinger complex. The sensitivity of I_{NaP} to hypoxia is well documented (Hammarstrom and Gage, 2002) including in pre-BötC inspiratory neurons (Koizumi and Smith, 2008). Repeated and persistent

episodes of hypoxia enhance I_{NaP} and likely induce overactivity in pacemaker neurons during this hypoxia. Here, we speculate that chronic overactivity induces a compensatory activity-dependent change in I_{NaP} in Pre-I/I neurons, which we model as a reduction of its conductance. It has been suggested that CIH conditioning enhances I_{NaP} in neonatal mouse slice but without consideration for animal sex (Garcia et al., 2017). In the past, we modeled CIH-induced plasticity in the context of male rats as an increase in the excitability of Pre-I/I pacemaker neurons (Barnett et al., 2017). This suggested mechanism was drawn from the observation that the leak conductance in spontaneously hypertensive rats is reduced in Pre-I/I neurons compared to control animals (Moraes et al.,

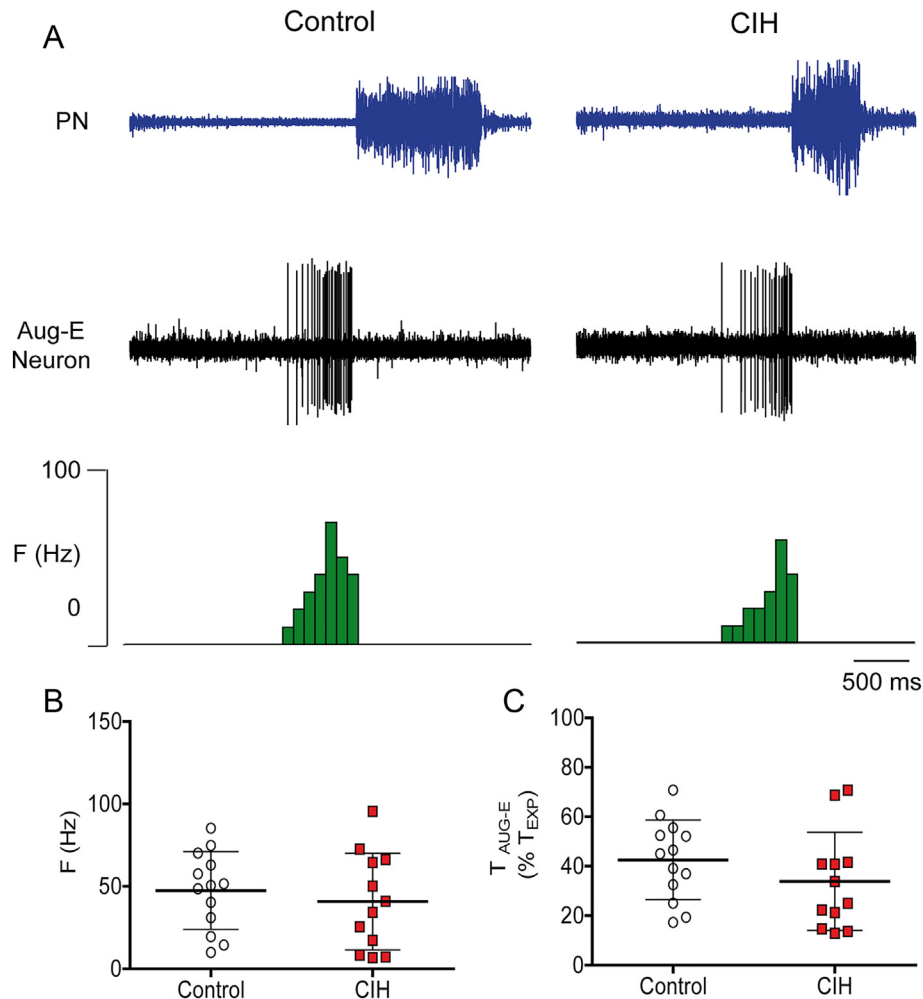


Fig. 10. Augmenting-expiratory neurons (Aug-E) activity in CIH-female rats. (A) Recordings of Aug-E neurons representative from control and CIH-female rats. Average and individual values from CIH ($n = 12$) and control ($n = 13$) group of Aug-E neurons firing frequencies (B) and the duration of activity relative to the duration of inspiratory phase (C). Values are mean \pm SD. Bin size = 100 ms.

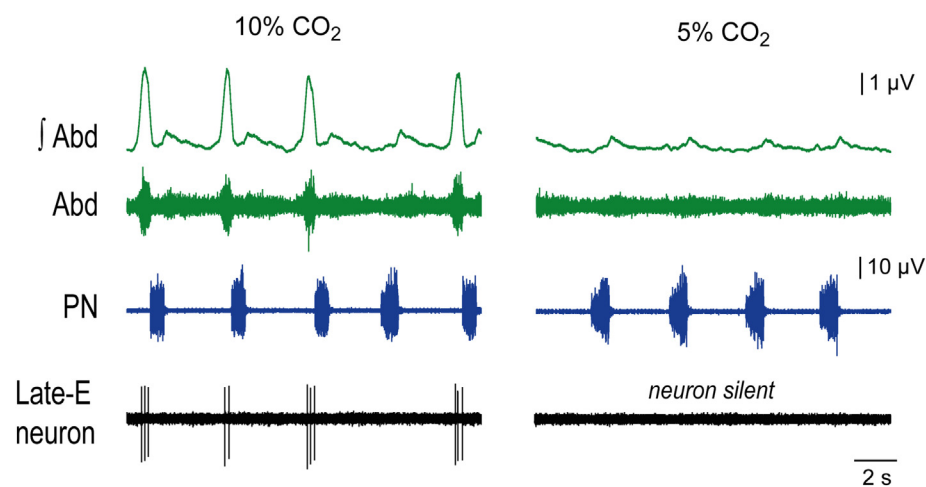


Fig. 11. Late-expiratory neurons (Late-E) activity in CIH-female rats. Recordings of a Late-E neuron in a CIH-female rat. Under hypercapnia in WHBP ($CO_2 = 10\%$) Late-E neurons CIH-female rats presented active expiration and Late-E neurons are active in this condition (left). However, under normocapnia condition in WHBP ($CO_2 = 5\%$), Late-E neurons expiration is passive and Late-E neurons are silent (right).

2014). Clear behavioral differences in male and female animals following CIH conditioning indicates that differential neurophysiological changes manifest during hypoxic conditioning. Our parsimonious hypothesis is that the excitability of Pre-I/I neurons is differentially regulated by CIH conditioning and male and female rats.

Considering alternate models

Here, we describe how CIH-induced plasticity in inspiratory pacemaker neurons of the pre-Bötzinger complex could lead to the loss of the “rampiness” of inspiratory-phase sympathetic motor output. However, this same interaction could be mediated by the projection of inhibitory Pre-I/I neurons directly to the RVLM. The plasticity that we describe (the reduction of persistent sodium current conductance) would be valid in this alternate model since the firing rate in the Pre-I/I population would still determine the magnitude of inspiratory inhibition. Our computational model contains two early inspiratory populations with an adapting pattern: Early-I (1) of the pre-Bötzinger complex, which participates in the respiratory central pattern generator and Early-I (2) of the rVRG, which interacts with Ramp-I neurons to produce their ramping pattern. Since each of these populations provides decrementing inhibition, it is straightforward to consider them as alternate sources of decrementing inhibition onto RVLM. However, each has its own drawback. Early-I (1) is critical for the expiration-to-inspiration phase transition, and perturbations that alter its firing rate dramatically alter the duration of expiration. Early-I (2) is responsible for the ramping pattern of the phrenic nerve; the loss of adaptation in this population would eliminate phrenic ramping, which would be inconsistent with experimental observation of CIH in female rats.

CONCLUSION

Sympathetic response to peripheral chemoreflex activation is enhanced in CIH-female rats. Carotid body ablation prevents

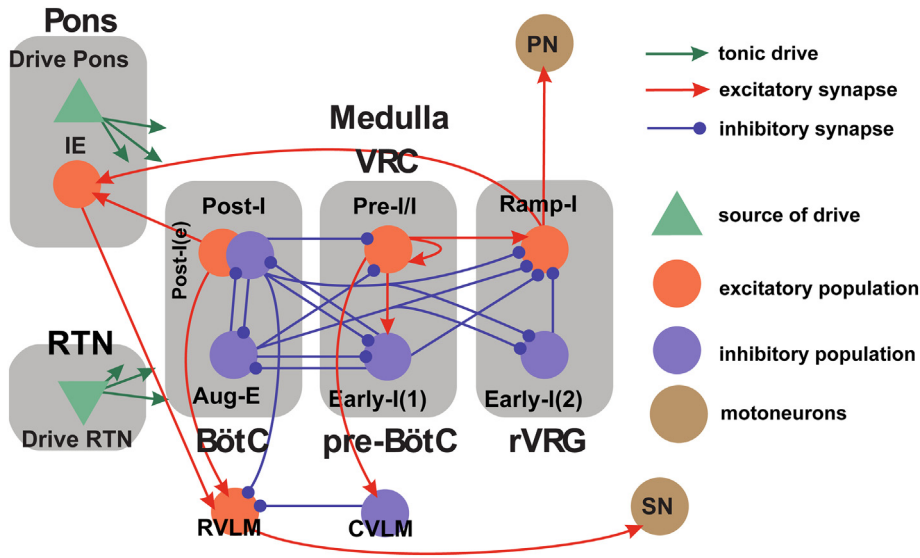


Fig. 12. Detailed connectivity diagram of our computational model. This model includes post inspiratory (Post-I) and augmenting expiratory (Aug-E) neurons of the Bötzinger complex; pre-inspiratory/inspiratory neurons (Pre-I/I) and early inspiratory (Early-I (1)) neurons of the pre-Bötzinger complex; ramping inspiratory (Ramp-I) and early inspiratory [Early-I (2)] neurons of the rostral ventrolateral respiratory group; phase spanning neurons (IE) of the pons; and finally rostral and caudal populations of the ventrolateral medulla (RVLM and CVLM). Excitatory and inhibitory populations are marked orange and blue respectively. Excitatory and inhibitory projections are marked red and blue respectively. Sources of tonic excitatory drive and their excitatory projections are marked in green. Motoneuron outputs – here the phrenic nerve (PN) and the sympathetic nerve (SN) – are marked brown. (For interpretation of the references to color in this figure legend, the reader is referred to the web version of this article.)

changes in the respiratory pattern and in the respiratory–sympathetic coupling in CIH-female rats. CIH induces changes in the respiratory network activity marked by a reduction in the Pre-I/I neuron firing frequency and prolongation of Post-I neuron activity. We conclude that intermittent activation of peripheral chemoreceptors during the time course of CIH drives changes of the respiratory network activity which ultimately influence the SNA leading to an enhanced inspiratory drive that produces sympathetic overactivity in CIH-female rats. Simulating the reduction in

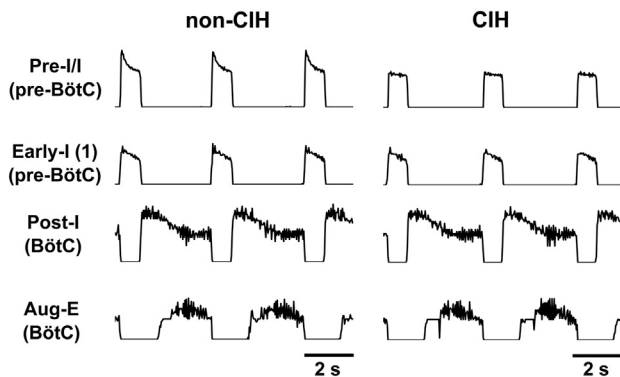


Fig. 13. Exemplar simulations of respiratory central pattern generator for non-CIH and chronic intermittent hypoxia (CIH) conditioned female rats. The traces represent the integrated population of firing rates. The population firing rates of the Pre-I/I and the Early-I populations of the pre-Bötzinger complex are depicted here as well as the activity of the Post-I and Aug-E populations of the Bötzinger complex.

Pre-I/I activity by decreasing I_{NaP} conductance was sufficient to reproduce the increase in inspiratory modulation of SNA. All together, these results contribute to a better understanding of the mechanisms by which CIH drives changes in respiratory–sympathetic network activity and possibly hypertension via chronic CBs activation in female rats.

Perspectives

There are relatively few studies exploring female physiology, specifically on the neural control of breathing and blood pressure. Recent studies suggest CBs removal as therapeutic target to treat drug-resistant hypertensive subjects. In this sense, the present study contributes to the idea that CBs ablation is sufficient to prevent autonomic and respiratory disorders in female rats exposed to CIH. Importantly, more information regarding female neurophysiology at the level of single respiratory neuron activity is

necessary taking into consideration that these neurons are associated with pathophysiological conditions, such as experimental hypertension. Here we explored the

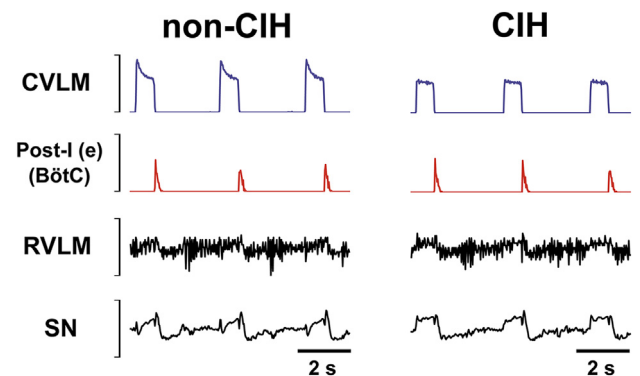


Fig. 14. The pre-sympathetic rostral ventrolateral medullary (RVLM) population is modeled to receive both excitatory and inhibitory inputs. An excitatory post-inspiratory population of the Bötzinger complex [Post-I (e)] provides input to the RVLM (trace depicted in red) that supports the post-inspiratory component of the sympathetic inspiratory/post-inspiratory burst. A caudal ventrolateral medullary (CVLM) population provides inhibitory input to the RVLM (trace depicted in blue). (Left Panel) In the non-CIH simulation, the CVLM has an adapting pattern during inspiration. This declining inhibition is visible as an inspiratory phase ramp in the sympathetic nerve activity (Right Panel). In the simulation of CIH in female rats, a reduction in the conductance of the intrinsic persistent sodium current is sufficient to reduce the Pre-I/I population firing rate and remove its adapting pattern, which drives CVLM. The change in shape of this input alleviates inhibition of the RVLM during the inspiratory phase, which abolishes the ramping shape of the SN.

extracellular activity of specific respiratory neurons subtypes in female rats exposed to CIH. Further investigation using intracellular or whole cell recordings of respiratory neurons in female rats is necessary to reveal the electrophysiological mechanisms involved in the altered firing properties of these neurons.

The physiological role of sex-differences in respiratory–sympathetic coupling after CIH remains unclear. In CIH-female rats, we speculate that the increase in SNA phase-locked to inspiration is related to an increase in blood flow to the lungs, optimizing the gas exchange during the inspiratory phase. In CIH-male rats, the increase in SNA could be related to the increase in blood flow during the late-expiration, optimizing the gas exchange during this phase of respiratory cycle, which is mainly related to removal of CO₂. It is possible that the respiratory and sympathetic networks of male and female rats are sexually dimorphic at the neuronal and network levels and respond differently to metabolic challenges such as CIH. Of note, sex differences in the respiratory modulation of sympathetic activity have been documented in humans (Wallin et al., 2010). However, the physiological role of these differences also remains elusive.

ACKNOWLEDGMENTS

This work was funded by Fundação de Amparo a Pesquisa do Estado de São Paulo (FAPESP, #2013/06077-5 to B.H.M. and #2015/06550-8 to G.M.P.R.S.), Conselho Nacional de Desenvolvimento Científico e Tecnológico (CNPq, #303512/2015-6 to BHM) and Coordenação de Aperfeiçoamento de Pessoal de Ensino Superior. Y.I.M and W.H.B are funded by NIH (grants: R01AT008632 and U01EB021960 to Y.I.M.).

COMPETING INTERESTS

None declared.

AUTHOR CONTRIBUTIONS

G.M.P.R.S, W.H.B, M.R.A, L.L, D.J.A.M, Y.I.M, B.H.M designed the research; G.M.P.R.S performed all the experiments with single unit neuronal and nerve recordings; G.M.P.R.S and M.R.A performed the experiments with carotid body removal; L.L. performed the patch-clamp experiments; W.H.B and Y.I.M. performed the computational modeling. G.M.P.R.S, L.L, W.H.B and Y.I.M analyzed the data; G.M.P.R.S, W.H.B, M.R.A, L.L, Y.I.M, B.H.M wrote the manuscript. All the authors approved the final version of the manuscript and agree to be accountable for all aspects of the work in ensuring that questions related to the accuracy or integrity of any part of the work are appropriately investigated and resolved. All persons designated as authors qualify for authorship, and all those who qualify for authorship are listed.

REFERENCES

Abdala APL, Koizumi H, Rybak IA, Smith JC, Paton JFR. (2007) The 3-2-1 state respiratory rhythm generator hypothesis revealed by microsectioning, reduced extracellular chloride and alterations in arterial gas tensions in the in situ rat. *FASEB J* 21:A557-A558.

- Abdala AP, McBryde FD, Marina N, Hendy EB, Engelman ZJ, Fudim M, Sobotka PA, Gourine AV, Paton JF. (2012) Hypertension is critically dependent on the carotid body input in the spontaneously hypertensive rat. *J Physiol* 590:4269-4277.
- Accorsi-Mendonca D, Machado BH. (2013) Synaptic transmission of baro- and chemoreceptors afferents in the NTS second order neurons. *Auton Neurosci* 175:3-8.
- Accorsi-Mendonca D, Castania JA, Bonagamba LG, Machado BH, Leao RM. (2011) Synaptic profile of nucleus tractus solitarius neurons involved with the peripheral chemoreflex pathways. *Neuroscience* 197:107-120.
- Accorsi-Mendonca D, Almado CE, Bonagamba LG, Castania JA, Moraes DJ, Machado BH. (2015) Enhanced firing in NTS induced by short-term sustained hypoxia is modulated by glia–neuron interaction. *J Neurosci* 35:6903-6917.
- Amorim MR, Bonagamba LG, Souza GM, Moraes DJ, Machado BH. (2016) Role of respiratory changes in the modulation of arterial pressure in rats submitted to sino-aortic denervation. *Exp Physiol* 101:1359-1370.
- Amorim MR, Bonagamba LGH, Souza G, Moraes DJA, Machado BH. (2017) Changes in the inspiratory pattern contribute to modulate the sympathetic activity in sino-aortic denervated rats. *Exp Physiol* 102:1100-1117.
- Baekey DM, Molkov YI, Paton JF, Rybak IA, Dick TE. (2010) Effect of baroreceptor stimulation on the respiratory pattern: insights into respiratory–sympathetic interactions. *Respir Physiol Neurobiol* 174:135-145.
- Barnett WH, Abdala AP, Paton JF, Rybak IA, Zoccal DB, Molkov YI. (2017) Chemoreception and neuroplasticity in respiratory circuits. *Exp Neurol* 287:153-164.
- Barnett WH, Jenkin SEM, Milsom WK, Paton JFR, Abdala AP, Molkov YI, Zoccal DB. (2018) The Kolliker–Fuse nucleus orchestrates the timing of expiratory abdominal nerve bursting. *J Neurophysiol* 119:401-412.
- Braga VA, Soriano RN, Machado BH. (2006) Sympathoexcitatory response to peripheral chemoreflex activation is enhanced in juvenile rats exposed to chronic intermittent hypoxia. *Exp Physiol* 91:1025-1031.
- Butera RJ.Jr, Rinzel J, Smith JC. (1999) Models of respiratory rhythm generation in the pre-Bötzinger complex. I. Bursting pacemaker neurons. *J Neurophysiol* 82(1):382-397.
- Caples SM, Gami AS, Somers VK. (2005) Obstructive sleep apnea. *Ann Intern Med* 142:187-197.
- Chitravanshi VC, Kachroo A, Sapru HN. (1994) A midline area in the nucleus commissuralis of NTS mediates the phrenic nerve responses to carotid chemoreceptor stimulation. *Brain Res* 662:127-133.
- Colombari E, Menani JV, Talman WT. (1996) Commissural NTS contributes to pressor responses to glutamate injected into the medial NTS of awake rats. *Am J Physiol* 270:R1220-R1225.
- Costa KM, Moraes DJ, Machado BH. (2013) Acute inhibition of glial cells in the NTS does not affect respiratory and sympathetic activities in rats exposed to chronic intermittent hypoxia. *Brain Res* 1496:36-48.
- Costa-Silva JH, Zoccal DB, Machado BH. (2012) Chronic intermittent hypoxia alters glutamatergic control of sympathetic and respiratory activities in the commissural NTS of rats. *Am J Physiol Regul Integr Comp Physiol* 302:R785-R793.
- Del Rio R, Moya EA, Iturriaga R. (2010) Carotid body and cardiorespiratory alterations in intermittent hypoxia: the oxidative link. *Eur Respir J* 36:143-150.
- Del Rio R, Moya EA, Iturriaga R. (2014) Carotid body potentiation during chronic intermittent hypoxia: implication for hypertension. *Front Physiol* 5:434.
- Del Rio R, Andrade DC, Lucero C, Arias P, Iturriaga R. (2016) Carotid body ablation abrogates hypertension and autonomic alterations induced by intermittent hypoxia in rats. *Hypertension* 68:436-445.
- Finley JC, Katz DM. (1992) The central organization of carotid body afferent projections to the brainstem of the rat. *Brain Res* 572:108-116.

- Fletcher EC, Lesske J, Behm R, Miller CC, Stauss H, Unger T. (1992) Carotid chemoreceptors, systemic blood pressure, and chronic episodic hypoxia mimicking sleep apnea. *J Appl Physiol* (1985) 72:1978-1984.
- Franchini KG, Krieger EM. (1993) Cardiovascular responses of conscious rats to carotid body chemoreceptor stimulation by intravenous KCN. *J Auton Nerv Syst* 42:63-69.
- Garcia AJ, Rotem-Kohavi N, Doi A, Ramirez JM. (2013) Post-hypoxic recovery of respiratory rhythm generation is gender dependent. *PLoS One* 8:e60695.
- Garcia AJ, Dashevskiy T, Khuu MA, Ramirez JM. (2017) Chronic intermittent hypoxia differentially impacts different states of inspiratory activity at the level of the preBotzinger complex. *Front Physiol* 8:571.
- Hammarstrom AK, Gage PW. (2002) Hypoxia and persistent sodium current. *Eur Biophys J* 31:323-330.
- Haselton JR, Guyenet PG. (1989) Central respiratory modulation of medullary sympathoexcitatory neurons in rat. *Am J Physiol* 256: R739-R750.
- Iturriaga R, Moya EA, Del Rio R. (2009) Carotid body potentiation induced by intermittent hypoxia: implications for cardiorespiratory changes induced by sleep apnoea. *Clin Exp Pharmacol Physiol* 36:1197-1204.
- Jasinski PE, Molkov YI, Shevtsova NA, Smith JC, Rybak IA. (2013) Sodium and calcium mechanisms of rhythmic bursting in excitatory neural networks of the pre-Bötzinger complex: a computational modelling study. *Eur J Neurosci*. 37(2):212-230, <https://doi.org/10.1111/ejn.12042>.
- Koizumi H, Smith JC. (2008) Persistent Na⁺ and K⁺-dominated leak currents contribute to respiratory rhythm generation in the pre-Bötzinger complex in vitro. *J Neurosci* 28:1773-1785.
- Lee EJ, Woodske ME, Zou B, O'Donnell CP. (2009) Dynamic arterial blood gas analysis in conscious, unrestrained C57BL/6J mice during exposure to intermittent hypoxia. *J Appl Physiol* (1985) 107:290-294.
- Machado BH. (2001) Neurotransmission of the cardiovascular reflexes in the nucleus tractus solitarius of awake rats. *Ann N Y Acad Sci* 940:179-196.
- Machado BH, Zoccal DB, Moraes DJA. (2017) Neurogenic hypertension and the secrets of respiration. *Am J Physiol Regul Integr Comp Physiol* 312:R864-R872.
- Mandel DA, Schreihofer AM. (2006) Central respiratory modulation of barosensitive neurones in rat caudal ventrolateral medulla. *J Physiol*. 572(Pt 3):881-896.
- McBryde FD, Abdala AP, Hendy EB, Pijacka W, Marvar P, Moraes DJ, Sobotka PA, Paton JF. (2013) The carotid body as a putative therapeutic target for the treatment of neurogenic hypertension. *Nat Commun* 4:2395.
- Molkov YI, Abdala AP, Bacak BJ, Smith JC, Paton JF, Rybak IA. (2010) Late-expiratory activity: emergence and interactions with the respiratory CpG. *J Neurophysiol* 104:2713-2729.
- Molkov YI, Zoccal DB, Moraes DJ, Paton JF, Machado BH, Rybak IA. (2011) Intermittent hypoxia-induced sensitization of central chemoreceptors contributes to sympathetic nerve activity during late expiration in rats. *J Neurophysiol* 105:3080-3091.
- Molkov YI, Bacak BJ, Dick TE, Rybak IA. (2013) Control of breathing by interacting pontine and pulmonary feedback loops. *Front Neural Circuits* 7:16.
- Molkov YI, Rubin JE, Rybak IA, Smith JC. (2017) Computational models of the neural control of breathing. *Wiley Interdiscip Rev Syst Biol Med* 9(2), <https://doi.org/10.1002/wsbm.1371>.
- Moraes DJ, Machado BH. (2015) Electrophysiological properties of laryngeal motoneurons in rats submitted to chronic intermittent hypoxia. *J Physiol* 593:619-634.
- Moraes DJ, Dias MB, Cavalcanti-Kwiatkoski R, Machado BH, Zoccal DB. (2012) Contribution of the retrotrapezoid nucleus/parafacial respiratory region to the expiratory-sympathetic coupling in response to peripheral chemoreflex in rats. *J Neurophysiol* 108:882-890.
- Moraes DJ, Zoccal DB, Machado BH. (2012) Sympathoexcitation during chemoreflex active expiration is mediated by L-glutamate in the RVLM/Bötzinger complex of rats. *J Neurophysiol* 108:610-623.
- Moraes DJ, da Silva MP, Bonagamba LG, Mecawi AS, Zoccal DB, Antunes-Rodrigues J, Varanda WA, Machado BH. (2013) Electrophysiological properties of rostral ventrolateral medulla presympathetic neurons modulated by the respiratory network in rats. *J Neurosci* 33:19223-19237.
- Moraes DJ, Machado BH, Paton JF. (2014) Specific respiratory neuron types have increased excitability that drive presympathetic neurones in neurogenic hypertension. *Hypertension* 63:1309-1318.
- Nanduri J, Semenza GL, Prabhakar NR. (2017) Epigenetic changes by DNA methylation in chronic and intermittent hypoxia. *Am J Physiol Lung Cell Mol Physiol* 313:L1096-L1100.
- Nanduri J, Peng YJ, Wang N, Khan SA, Semenza GL, Prabhakar NR. (2018) DNA methylation in the central and efferent limbs of the chemo reflex requires carotid body neural activity. *J Physiol* 596 (15):3087-3100, <https://doi.org/10.1113/JP274833>.
- Narkiewicz K, van de Borne PJ, Cooley RL, Dyken ME, Somers VK. (1998) Sympathetic activity in obese subjects with and without obstructive sleep apnea. *Circulation* 98:772-776.
- Narkiewicz K, van de Borne PJ, Montano N, Dyken ME, Phillips BG, Somers VK. (1998) Contribution of tonic chemoreflex activation to sympathetic activity and blood pressure in patients with obstructive sleep apnea. *Circulation* 97:943-945.
- Narkiewicz K, Ratcliffe LE, Hart EC, Briant LJ, Chrostowska M, Wolf J, Szyndler A, Hering D, Abdala AP, Manghat N, Burchell AE, Durant C, Lobo MD, Sobotka PA, Patel NK, Leiter JC, Engelman ZJ, Nightingale AK, Paton JF. (2016) Unilateral carotid body resection in resistant hypertension: a safety and feasibility trial. *JACC Basic Transl Sci* 1:313-324.
- Oliveira-Sales EB, Colombari E, Abdala AP, Campos RR, Paton JF. (2016) Sympathetic overactivity occurs before hypertension in the two-kidney, one-clip model. *Exp Physiol* 101:67-80.
- Paton JF, Abdala AP, Koizumi H, Smith JC, St-John WM. (2006) Respiratory rhythm generation during gasping depends on persistent sodium current. *Nat Neurosci* 9:311-313.
- Pierrefiche O, Champagnat J, Richter DW. (1995) Calcium-dependent conductances control neurones involved in termination of inspiration in cats. *Neurosci Lett* 184:101-104.
- Pijacka W, McBryde FD, Marvar PJ, Lincevicius GS, Abdala AP, Woodward L, Li D, Paterson DJ, Paton JF. (2016) Carotid sinus denervation ameliorates renovascular hypertension in adult Wistar rats. *J Physiol* 594:6255-6266.
- Pijacka W, Moraes DJ, Ratcliffe LE, Nightingale AK, Hart EC, da Silva MP, Machado BH, McBryde FD, Abdala AP, Ford AP, Paton JF. (2016) Purinergic receptors in the carotid body as a new drug target for controlling hypertension. *Nat Med* 22:1151-1159.
- Prabhakar NR, Semenza GL. (2015) Oxygen sensing and homeostasis. *Physiology* (Bethesda) 30:340-348.
- Prabhakar NR, Peng YJ, Jacono FJ, Kumar GK, Dick TE. (2005) Cardiovascular alterations by chronic intermittent hypoxia: importance of carotid body chemoreflexes. *Clin Exp Pharmacol Physiol* 32:447-449.
- Richter DW, Smith JC. (2014) Respiratory rhythm generation in vivo. *Physiology* (Bethesda) 29:58-71.
- Rybak IA, Shevtsova NA, Paton JF, Dick TE, St-John WM, Morschel M, Dutschmann M. (2004) Modeling the ponto-medullary respiratory network. *Respir Physiol Neurobiol* 143:307-319.
- Rybak IA, Molkov YI, Paton JFR, Abdala AP, Zoccal DB. (2012) Chapter 143 — modeling the autonomic nervous system. In: David R, Italo B, Geoffrey B, Phillip AL, & Julian FRP, editors. *Primer on the autonomic nervous system*. San Diego: Academic Press. p. 681-687.
- Rybak IA, Molkov YI, Jasinski PE, Shevtsova NA, Smith JC. (2014) Rhythmic bursting in the pre-Bötzinger complex: mechanisms and models. *Prog Brain Res*. 209:1-23, <https://doi.org/10.1016/B978-0-444-63274-6.00001-1>.
- Sasaki N, Nagai M, Mizuno H, Kuwabara M, Hoshida S, Kario K. (2018) Associations between characteristics of obstructive sleep apnea and nocturnal blood pressure surge. *Hypertension* 72:1133-1140.
- Schreihofer AM, Guyenet PG. (2002) The baroreflex and beyond: control of sympathetic vasomotor tone by GABAergic neurons in the ventrolateral medulla. *Clin Exp Pharmacol Physiol*. 29(5-6):514-521.

- Shortt CM, Fredsted A, Chow HB, Williams R, Skelly JR, Edge D, Bradford A, O'Halloran KD. (2014) Reactive oxygen species mediated diaphragm fatigue in a rat model of chronic intermittent hypoxia. *Exp Physiol* 99:688-700.
- Smith JC, Abdala AP, Koizumi H, Rybak IA, Paton JF. (2007) Spatial and functional architecture of the mammalian brain stem respiratory network: a hierarchy of three oscillatory mechanisms. *J Neurophysiol* 98:3370-3387.
- Somers VK, Dyken ME, Clary MP, Abboud FM. (1995) Sympathetic neural mechanisms in obstructive sleep apnea. *J Clin Invest* 96:1897-1904.
- Souza GM, Bonagamba LG, Amorim MR, Moraes DJ, Machado BH. (2015) Cardiovascular and respiratory responses to chronic intermittent hypoxia in adult female rats. *Exp Physiol* 100:249-258.
- Souza GM, Bonagamba LG, Amorim MR, Moraes DJ, Machado BH. (2016) Inspiratory modulation of sympathetic activity is increased in female rats exposed to chronic intermittent hypoxia. *Exp Physiol* 101:1345-1358.
- Souza GMPR, Amorim MR, Moraes D.J.A., Machado B.H.. (2018) Sex differences in the respiratory-sympathetic coupling in rats exposed to chronic intermittent hypoxia. *Respir Physiol Neurobiol* 256:109-118, <https://doi.org/10.1016/j.resp.2017.09.003>.
- Stevens CF, Wang Y. (1994) Changes in reliability of synaptic function as a mechanism for plasticity. *Nature* 371:704-707.
- St-John WM, Paton JF. (2003) Respiratory-modulated neuronal activities of the rostral medulla which may generate gasping. *Respir Physiol Neurobiol* 135:97-101.
- Tubek S, Niewinski P, Reczuch K, Janczak D, Rucinski A, Paleczny B, Engelman ZJ, Banasiak W, Paton JF, Ponikowski P. (2016) Effects of selective carotid body stimulation with adenosine in conscious humans. *J Physiol* 594:6225-6240.
- Wallin BG, Hart EC, Wehrwein EA, Charkoudian N, Joyner MJ. (2010) Relationship between breathing and cardiovascular function at rest: sex-related differences. *Acta Physiol (Oxf)* 200:193-200.
- Zoccal DB, Simms AE, Bonagamba LG, Braga VA, Pickering AE, Paton JF, Machado BH. (2008) Increased sympathetic outflow in juvenile rats submitted to chronic intermittent hypoxia correlates with enhanced expiratory activity. *J Physiol* 586:3253-3265.

(Received 9 November 2018, Accepted 19 March 2019)
(Available online 28 March 2019)